Local optimization of CLT floors

Optimization of Cross Laminated Timber floors through locally varying the major direction based on the geometry, support and loading conditions

Staat, Vincent B.

Award date:
2023

Local optimization of CLT floors

Optimization of Cross Laminated Timber floors through locally varying the major direction based on the geometry, support and loading conditions

Final Mater Thesis

V.B. Staat

Eindhoven University of Technolgy

Eindhoven, June 2023

Title	Local optimization of CLT floors
Subtitle	Optimization of Cross Laminated Timber floors through locally varying the major direction based on the geometry, support and loading conditions
Date	24-05-2023
Location	Eindhoven, Netherlands
Author	V.B. (Vincent) Staat
Student ID	1255134
Email	v.b.staat@student.tue.nl
Department	Built environment
Master	Architecture, Building and Planning
Master track	Structural Engineering and Design
Chair	Innovative Structural Design (ISD)
Graduation committee	Ir. A.P.H.W. Habraken | Assistant professor ISD Dr. Ir. S. P. G. Moonen | Associate professor ISD Ir M. T. Ferguson | Education/research officer ISD

Summary

The construction industry is a long way away from being energy neutral. As part of the Paris agreement the construction industry should be energy neutral by 2030. To achieve this, it is necessary to step away from conventional materials like steel and concrete and transition towards the use of green and bio-based materials. Timber is a good substitute for steel or concrete as modern advancement like laminating make it possible to achieve the same types of large-scale structures commonly build with concrete or steel. To generate more knowledge on timber in the industry and to emphasize the potential of timber this research was focused on developing an optimization algorithm to locally optimize cross laminated timber (CLT) floors. The aim is to generate significant material savings compared to conventional CLT by locally varying the major and minor direction in the floors.

The optimization is performed by dividing a floor into zones. To change the major direction of a zone the planks in the outer two layers at the top and bottom are rotated. This way, the planks in the outer layers run in a different direction (the new major direction) while the layers one step inward are rotated in the other direction (the new minor direction) to still provide sufficient load bearing capacity in this direction. The optimization principle is not possible for 3-ply CLT floors. For 5, 7, 9 and more ply floors the method ensures there are always continuous layers throughout the floor to make sure the floor can still structurally function as a whole.

Using the parametric scripting software Rhino Grasshopper in combination with the structural analysis software plugin Grasshopper GSA floors with different geometries, loads and supporting conditions can be analyzed. Based on the analysis results it is determined for each zone what the major direction should be. After this, the bending stresses and shear stresses in two directions are checked for each floor under ULS loading conditions. Additionally, the maximum deflections of the floor are checked relating to their relevant span distance between supports under SLS loading conditions. If any of the stress or deflection requirements are not met, the thickness of each layer in the floor is increased with 5 mm. When all layers of a floor are 40mm thick the next step is to add two more layers and start increasing the thickness of all layers again until they are 40mm. This is repeated until the minimum required thickness of the floor is found. The system can also be used without rotating zones which leads to the minimum required thickness for a conventional CLT floor.

By performing three case studies it was found that for theoretical material savings of up to 25% are possible using the optimization algorithm. There are also floors for which the optimization is not suited as not all types of floors can be optimized using the proposed optimization method.

An optimized floor cannot be made in a conventional CLT factory unless some adaptations are made to the assembly line. No new types of machines or robots are required to assemble the optimized floors however, so it is expected that it is feasible for a conventional factory to adapt to making optimized floors.

The research presents an optimization algorithm that can lead to significant theoretical material savings. Using a FEM analysis, it was found that the optimization technique can lead to large stresses perpendicular to the grain. This shows that further research and experiments are required on the optimized floors to determine the feasibility of the proposed optimization technique. The algorithm can be adapted to a different optimization technique as the basic logic of the script will not change. To locally optimize a floor, zones need to be found where the major direction should change after which all stresses need to be checked.

Contents

1

Introduction and problem statement and objective

It is widely known that the construction industry is responsible for around 40% of the global CO2 emission (IEA, 2019). This means that if the construction industry can change its emission numbers, it would have a significant effect on the world. One of the many ways to make these changes is to use carbon neutral and bio-based construction materials like timber. It was shown that constructing a building out of timber as opposed to concrete could reduce the CO2 emission of construction, use and demolition of the building by up to 42% (Liu, Guo, Sun, & Chang, 2016, p9). In the research by Liu et al. (2016) a case study was done for a building in Harbin, China. In the winter it gets extremely cold in Harbin, and it was found that the natural isolation properties of timber would drastically lower the energy consumption during the winter compared to a concrete building. Timber is not only a greener material to produce (provided it is obtained through sustainable forest management) but this study shows that during the use of the building timber reduces energy consumption as well.

When looking at timber construction products Cross Laminated Timber (CLT) is a popular choice as it makes it possible to make large scale, multiple story building out of timber (HAUT Amsterdam, 2022). The use of CLT is however not yet at a level where it is fully replacing concrete building methods. When looking at a study performed by Penfield, Germain, Smith, & Stehman (2022, p1) it can be concluded that a large number of parties concerned with construction have a lack of experience with CLT. This could be an explanation for the lacking use of CLT in construction. Additionally, Penfield et al. (2022) found that a lack of tools and training make CLT unattractive for construction stakeholders. This shows that there is a need for research and development in CLT to stimulate its use in construction and make it a more attractive construction method.

CLT is manufactured by laminated timber in layers where each layer is rotated 90o compared to the previous one. This layered stacking of timber gives CLT panels two load bearing directions. This makes them good alternatives for concrete slabs for example. However, a CLT panel will always have a major and a minor direction. This is because a CLT panel will always need a symmetrical cross-section and thus have an odd number of layers (Wallner-Novak, Koppelhuber, & Pock, 2014, p2). Therefore, will always have more layers in one direction than in the other. For scenarios where there are a distinct major and minor direction in the flow of forces CLT is highly suitable. Think of floors supported on two opposing sides. However, when there is no clear major direction for the flow of forces throughout the entire floor, like a point supported floor, CLT can show its weakness. The required thickness of the floor can be governed by local stresses and deflections in the minor direction of the floor. The aim of this research is to set up an optimization algorithm that can locally vary the major and minor direction of a floor. This optimization will be achieved by varying the direction of planks in a single layer. The optimization algorithm will have to detect in which parts of the floor the planks should be rotated so the major direction is changed. This objective leads to the following research question:

In what way can an optimization algorithm be set up that can optimize a CLT floor by locally changing the major and minor direction of a floor based on the geometry of the floor, the support conditions, and the applied loading?

The aim of the research is to set up an optimization tool that can optimize all sorts of floors. This means it should work for various geometries, loads, and supports. The optimization tool will need to present a plank layout for a floor that satisfies the required stress and deflection requirements.
There have already been studies on the optimization of CLT floors. Two of these studies looked at removing timber from CLT and essentially creating a hollow core CLT floor leading to around 20% material reduction (Mayencourt & Mueller, 2019, p7-8; Moberg & Xiao, 2022, p165-168). Another study looked at CLT floors strengthened with vertical ribs in the bottom layer. In this study it was found that up to 50% material can be saved compared to conventional CLT (Sustersic, 2016, p9). Due to the added ribs the total thickness of the floor package is significantly increased. These studies show that CLT has potential for optimization, but all these studies have only looked at optimizing floors in the same way for the whole floor. The optimization is based on a global level for the element and not a local level. Therefore, the optimization system in this study will have to be set up from scratch. Locally defining optimization zones must be done using an algorithm as it would be very time consuming to determine the optimization pattern of a floor by hand. The aim of this research is to set up an algorithm that is easy to use and can quickly show the optimization results for various types of floors. Where the previous studies have mainly focused on the structural performance of the established optimization technique, this study will mostly focus on the development of the optimization algorithm. Only after this algorithm is set up and optimized floor design can be found, can the structural performance of these floors be studied. This research will form a starting point from which the newly developed optimization technique can be further studied and improved.

2
CLT as a material

2.1: CLT structural behavior

Cross laminated timber (CLT) is the act of making mass timber floors and walls by gluing layers of sawn timber on top of each other in which every other layer is rotated by 90o. CLT was developed in the mid 1990-s but only in the early 2000s construction with CLT started to increase (FP innovations, 2020, p2). The high strength, good structural performance and stability, and the ability to be produced quickly and prefabricated makes CLT a suitable alternative for materials like concrete and masonry (Pereira & Calil Junior, 2019, p2)

Due to the cross-wise stacking of CLT the panels have relatively high in-plane and out -of-plane strength and stiffness giving the panels two-way action capabilities like a reinforced concrete slab (FP innovations, 2020, p8). CLT panels are however always made using and odd number of layers to superficially form a homogenous wooden panel (Wallner-Novak, Koppelhuber, & Pock, 2014, p2). This means that CLT panels always have a major and a minor direction.

The individual planks in CLT are made by finger jointing shorter planks. The planks in a single layer can be glued together which is called edge bonding. Edge bonding allows for transfer of stresses between adjacent planks and creates a more uniform layer which can enhance the physical properties like air tightness, fire resistance and acoustic performance (Thiel, 2013, p86; Püssa & Kers, 2017, p15). A disadvantage of edge bonding besides the increased production complexity is that it can cause irregular crack formation in a panel due to shrinkage and swelling as illustrated in figure 1 (Brandner, 2014, p11).

Due to the layered orthotropic nature of CLT the stress distribution in CLT is unique. The large difference in strength between the direction parallel and perpendicular to the grain in timber(11000 MPa against 370 MPa for C24 timber (NEN, 2016, p10)) causes the perpendicular layers to remain relatively unstressed. Calculation methods even propose to set the E-modulus of perpendicular layers (E_{90}) to zero. This is because in addition to the large stiffness difference, normal stresses can almost not be transferred in the cross layers between adjacent planks due to regular gaps and cracks in the boards (Thiel, 2013, p86). These effects cause the bending stress distributions in the two directions of the panel to be as shown in figure 2.

When considering shear stresses all the layers are able to transfer stresses, so the stress distribution is not as step-wise as previously shown for bending. However, cross layers of a cross section are subject to rolling shear: the grains in the plank can start rolling over each other. This effect is illustrated in figure 3 (Pereira & Calil Junior, 2019, p5)

The rolling shear stiffness of timber is significantly lower than the transverse shear stiffness (0.8 MPa against 3.5 MPa (NEN, 2016, p10). This causes the stresses to minimally increase in cross layers but still be transferred through these layers. The simplified (taking $E_{90} = 0$) shear stress distribution in a CLT panel is illustrated in figure 4.

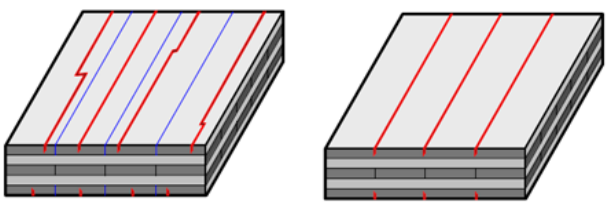

Figure 1: Crack formation (red) during shrinkage and swelling for edge bonding (left) en no edge bonding (right) (Brander, 2014, p11)

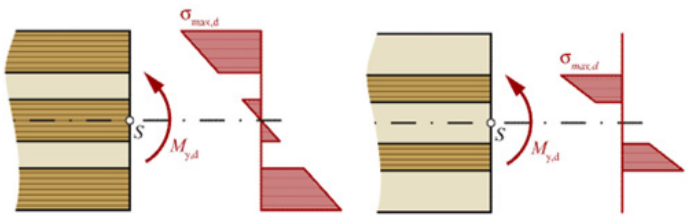

Figure 2: Bending stress distribution in CLT in major (left) and minor (right) direction (Thiel, 2013, p86)

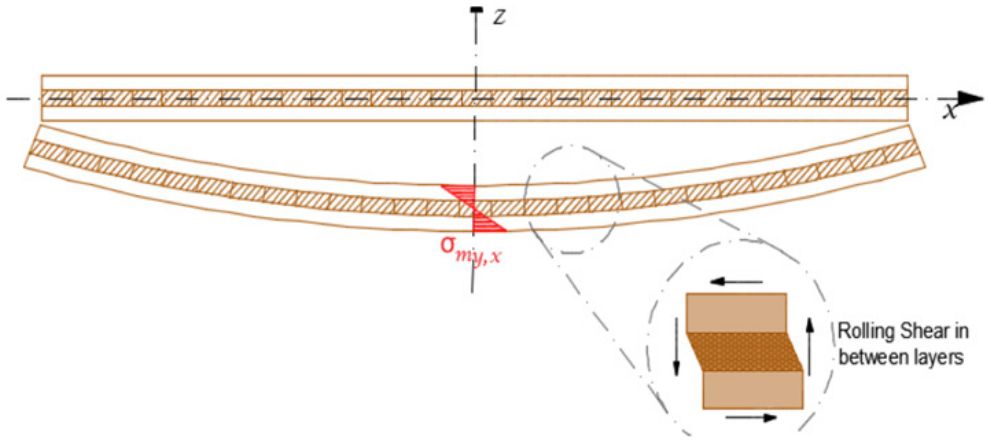

Figure 3: Rolling shear as effect of bending in CLT (Pereira & Calil Junior, 2019, p5)

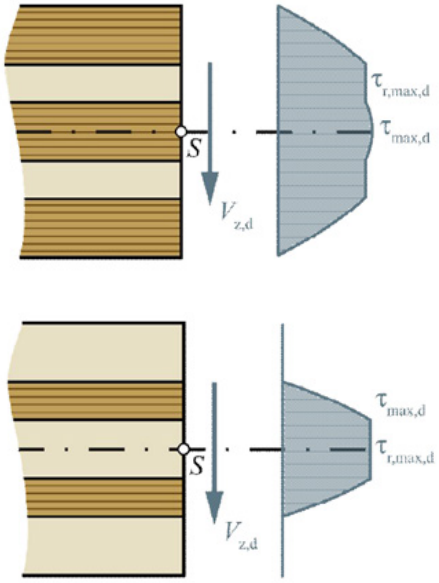

Figure 4: Shear stress distribution in CLT for major (left) and minor (right) direction (Thiel, 2013, p94)

The rolling shear strength of timber is significantly lower than the transverse shear strength of timber. This causes rolling shear failure to be one of the governing failure modes of CLT alongside glue line failure (delamination) and tension failure (Mohd Yusof, Md Tahir, Lee, Khan, & Mohammad Suffian James, 2019, p8).

Timber is a highly orthotropic natural material causing variance in its properties. Alongside the natural variance there can always be knots or other defects in timber. Layering and gluing of such a material result in a complex composite. As discussed above the stress distribution and failure behavior of CLT is complex and requires attention when designing and calculating CLT. Still, CLT is a promising structural material as it can be a bio-based and sustainable alternative to prefab concrete construction. CLT panels can often reach the structural capabilities of concrete slabs at a way lower density. This is beneficial as it means the building can be lighter resulting in a smaller foundation and easier and faster construction. On the other hand, the low mass of CLT makes it so that it often does not comply easily to acoustic requirements, requiring additional mass to be placed on the floor (RISE Research Institutes of Sweden, 2019, p102). To illustrate the capabilities of CLT a few reference projects have been highlighted in the following section.

2.2 CLT applied: Haut

Haut is a 73-meter tall, 21 story timber apartment building in Amsterdam. It is constructed using glue laminated timber columns and CLT floors and walls. The foundation, basement and core are made using concrete. (Arup, n.d.)

Figure 5: Haut Amsterdam (Arup, n.d.)

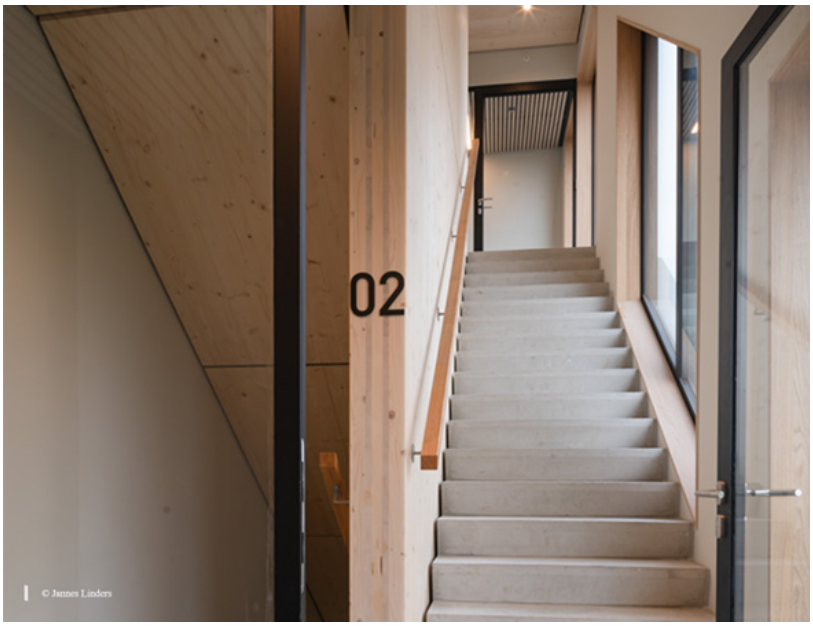

Figure 6: Stairwell in Haut, Amsterdam (Arup, n.d.)

2.3 CLT applied: Dalston works

The Dalston works project located in London and designed by Waugh Thistleton Architects is one of the largest full CLT constructions. All the walls and floors are made using CLT. A masonry façade cladding replaces the natural timber look with that of a more traditional building. The project highlights the capability of using CLT for high density urban housing and fast construction (Walsh, 2018).

Figure 7: Dalston works, London (walsh, 2018)

Figure 8: Dalston works during construction, London (walsh, 2018)

2.4 CLT applied: Asumma housest

Asumma is a Finish construction technology company that designs and builds single houses using CLT. Their projects highlight the precise prefabrication tolerances allowing direct placement of doors and windows. Additionally, their projects show the fast construction process of building with CLT. The house shown in figure 9 below was assembled in only 2 days (Mela, 2023).

Figure 9: CLT dwelling by Asumma in construction (Mela, 2013)

The reference projects discussed show the versatility and the capability of constructing with CLT. It shows that, despite the drawbacks and increased complexity of CLT, it is already possible to replace concrete with timber and thereby drastically lowering the embodied energy and carbon of a building. The largest drawback of CLT that this research will focus on is the strong major and minor direction of CLT panels.

3
Optimization principle

Now that the behavior and properties of CLT have been elaborated it will be discussed how the CLT panels are aimed to be optimized. This chapter will go over the possible strategies of locally varying the major and minor direction of a CLT panel to have it be more in line with the load and supporting conditions of the panel while keeping the panel and layer thickness constant throughout the floor.

The aim of the optimization of CLT floors is to reduce the required amount of material (thickness of the floors) to meet the structural and serviceable limits by locally changing the major direction of the floors. Figure 10 shows a regular 5 ply CLT floor with its major direction being in the x direction indicated in the figure. The floor is divided into rectangular zones. In reality these zones are not visible as the planks in each layer run continuous in their major direction through finger joints. The optimization will look at the stresses in each zone of the floor and thereby determine if the major direction of each zone will have to be rotated. The size of these zones should ideally be equal to squares the size of the width of the used planks. The size can be taken larger or smaller, but this will create challenges during production as some planks will then have to be made less wide along their length to fit them between other zones.

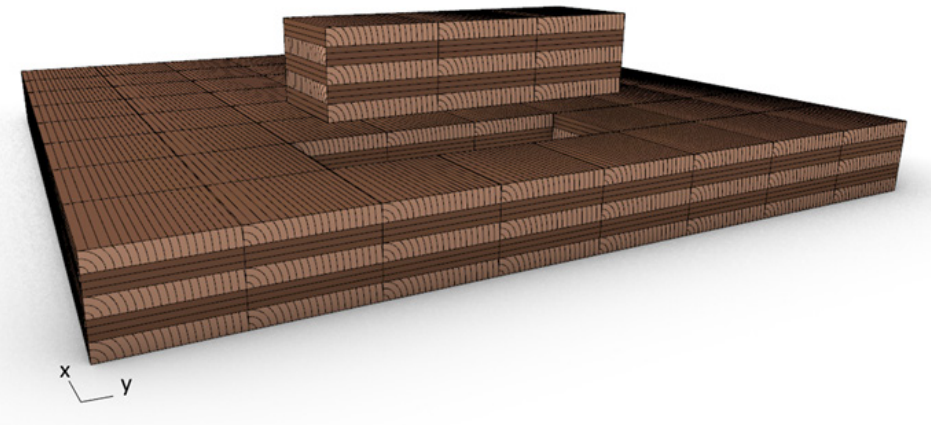

Figure 10: Conventional 5 ply CLT floor

A first idea to change the major direction of the floor could be to simply rotate an entire zone as visualized in figure 11. This will however cause problems when looking at how these zones will work in the floor. When all layers in a zone are rotated it means that these zones are fully separate from the rest of the floor: there is no continuous layer of timber throughout the entire floor. This would mean that the parts of the floor only structurally work together through vertical glued connections between the edges of the zones. It is expected that a system like this would drastically decrease the total capacity of the floor and thus not optimize the floor.

Another solution is to only rotate the outer-most layers of the floor (figure 12). For a 5-ply floor this would mean that there are still three layers running continuously throughout the floor. This method of rotating would drastically increase the capacity of the original minor direction by having four of the five layers in the floor run in this direction. This will however create a problem in the other direction as there is only one layer left in this direction. While the optimization will be based on major stress directions, it will likely be the case that there will always be stresses in both directions in the floor. It will thus likely become problematic that only a single layer must be able to withstand the stresses in its direction after rotating. Since this layer is located in the middle of the floor package it would essentially create a single layer thick cross-section.

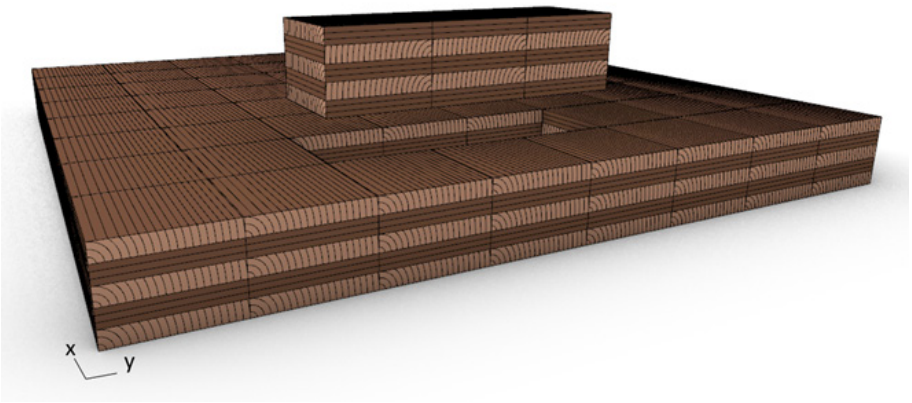

Figure 11: 5 ply CLT with three fully rotated zones

Figure 12: 5 ply CLT floor with only the outer layers rotated

To solve this problem the proposed way of rotating planks in a zone is visualized in figure 13. The two outer-most layers at the top and bottom of the floor will be rotated. This means that after rotation there are still only two layers running in the old minor direction. However, as these layers are at the outside of the floor package, they are structurally the most effective. This means that after rotating the major direction is still changed while there are still sufficient layers left running in the other direction. For a five ply CLT floor this would mean that the middle layer of the floor is continuous throughout the floor ensuring the floor will still function as a single structural element. For more plies there will be even more continuous layers. The choice to have at least one continuous layer in the floor means that the optimization process will not work for 3-ply CLT floors. If only the outer layers are rotated there will be no plies left in on direction. Additionally, if the outer layers are rotated but the center layer is rotated the other direction there will be layers running in both directions but there will not be a continuous layer in the floor anymore.

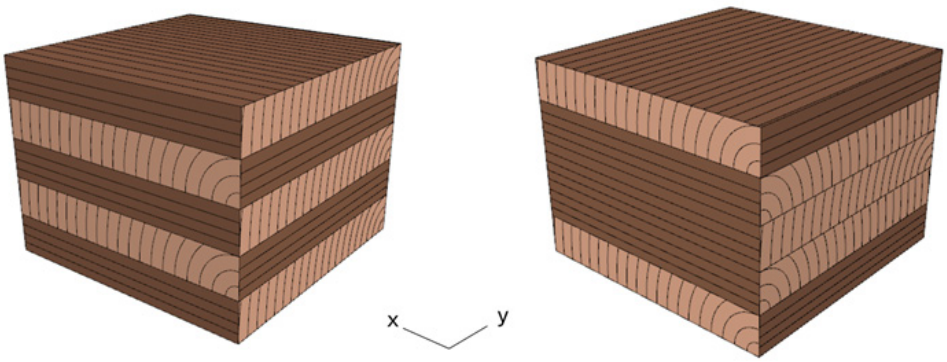

Figure 13: Proposed optimization method where the outer two layers at the top and bottom are rotated

Figure 14 shows the non-rotated and rotated y-direction cross sections for a 5, 7 and 9 ply floor showing how the minor cross section becomes the major cross section. For a 5-ply floor there is only a single continuous layer while the 7 and 9 ply floors have 3 and 5 continuous layers respectively. This is again because only the outer two layers at the top and bottom of the floor are rotated.

The effect of a rotation strategy like this on the stress distribution in a 5-ply floor has been visualized in figure 15 to 18 below.

The bending stresses in the Y-direction will be decreased as the effective layers are moved away from the center of the cross section. For the X-direction the opposite is happening. It is therefore important that during the optimization algorithm it is checked that rotating fixes a stress problem in the y-direction but does not simultaneously create a stress problem in the x-direction.

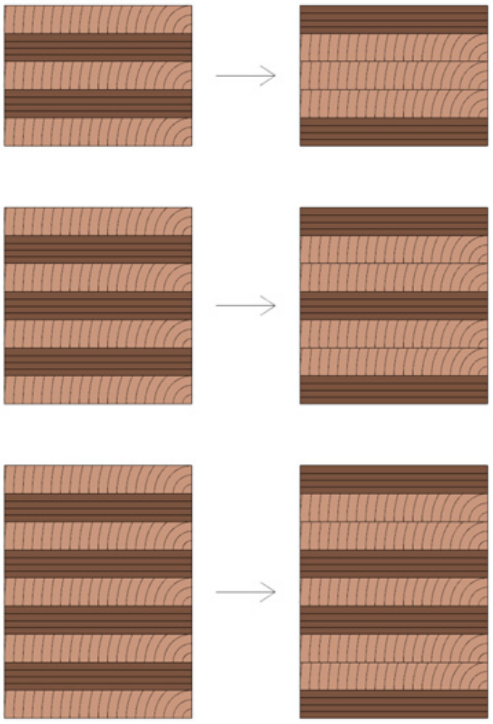

Figure 14: Optimization method shown for 5, 7 and 9 ply CLT floors

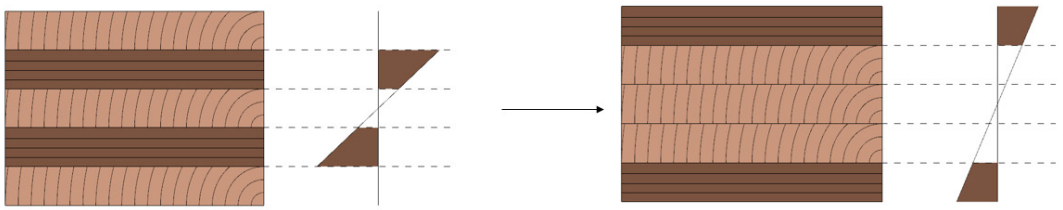

Figure 15: Bending stress redistribution in original major (x) direction

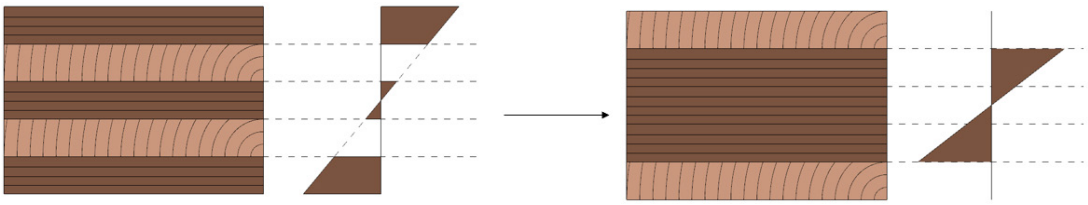

Figure 16: Bending stress redistribution in original minor (y) direction

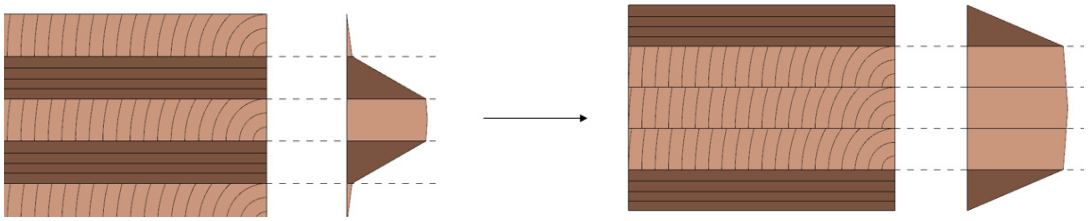

Figure 17: Shear stress redistribution in original major (x) direction

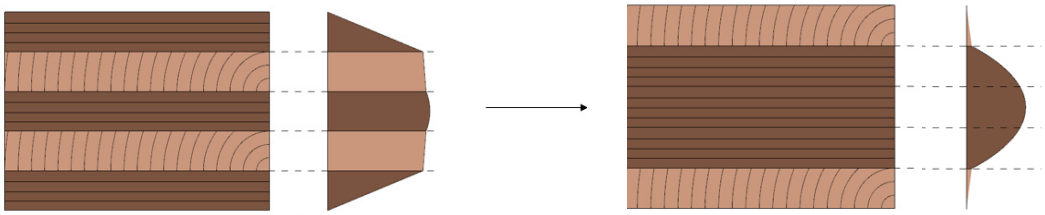

Figure 18: Shear stress redistribution in original minor (y) direction

For the shear stresses a similar phenomenon is happening where the stresses are decreased as the effective material is in the outer most layers. Due to the low stiffness of the timber in its minor direction the stresses will not increase significantly in the middle three layers. The highest stress will however occur in the middle layer which needs to be checked with the rolling shear strength of the used timber. In the X-direction we again see an increase in maximum stress. This maximum stress is located at the center of the cross section where the planks run in the strong direction. This means that the regular shear capacity of the timber must be checked which is significantly higher than the rolling shear strength (NEN, 2016, p10).

During the optimization a floor will be divided into zones. As mentioned before these zones are rectangles with length and width equivalent to the width of the planks used in the CLT floor. For each of these zones it will be determined in which direction the stresses are the highest. If the stresses are highest in the x-direction the zone does not have to be rotated. If the stresses are too high in this x-direction it means the floor has to become thicker. If the stresses in the y-direction are the largest, it means the zone should be rotated to favor the stress distribution. If after rotating the stresses are still too high in either direction, the floor needs to become thicker. The stresses are used to determine if a zone should be rotated or not. If after rotating the deflection is still beyond the set limits, the floor thickness should also be increased. When increasing the thickness of the floor the same zones will remain rotated. This means that the algorithm does not start with a regular CLT floor each time the thickness is increased. It increases the thickness of the rotated and non-rotated zones at the same time.

For the optimization algorithm it was chosen to have an identical layer thickness for all layers in the CLT. Changing the thickness of individual layers could affect the minor and major direction of the floor as well, but to reduce the complexity of the algorithm this was not included. Another strategy that is not included in the algorithm yet is rotating more layers for floors with more plies. Again, to reduce complexity of the algorithm this is not included but it is an interesting feature to research. For 9-ply CLT, only rotating the two outer most layers will have a relatively smaller effect on the performance of the floor as it will have for a 5-ply floor. It is expected that including this feature would make the optimization more effective for floors with a higher number of layers.

Now that optimization strategy is established it is possible to create an overview of the tools and methods that will be used to create an algorithm that can automatically apply this kind of optimization. As has been described above, choices have been made to make sure to algorithm did not become too complex. It is expected that changing the optimization strategy by expanding the features will lead to even more significant optimizations.

4

Optimization tools and methods

4.1 Rhino Grasshopper

The first and main software that is used is Rhino 3D in combination with the integrated parametric design plugin Grasshopper. This software allows for parametric visual programming. Grasshopper is used to make the algorithm in. All other tools and methods were chosen such that they are compatible with Grasshopper and therefore compatible with the algorithm. Rhino Grasshopper is commonly used as a parametric and generative design tool to create complex or optimized three-dimensional geometries. However, for the CLT optimization algorithm there won't be complex three-dimensional geometries. The input for the algorithm is the floor shape and size which is directly given in Grasshopper. From there on Grasshopper is mostly used for its data management and structuring methods in the rest of the algorithm to generate the optimized floors. The output of the algorithm is a plank layout for the outer layers including maximum stress and deflection values at critical locations in the floor.

4.2 GSA

The first step in the algorithm is to calculate the moments, shear forces and deflections in the floors. There are software packages that are especially made for calculating CLT. One of these software packages was developed at the University of Graz and is named CLT designer. CLT designer is a simple and fast software that calculates CLT floors as wide beams. It can be used to quickly determine the moments, forces, and stresses in CLT floors but is limited to solid floors (no openings) that are line supported on opposing edges. CLT designer cannot easily be coupled to Grasshopper and its limited floor geometry and support conditions do not make it a good fit for the algorithm. The software is however used for various cases to verify the calculation results of the algorithm. Another established software for calculating CLT is the FEM software Dlubal RFEM with the RF-Laminate plug-in. In this software the user can define a composite material lay-up that can be applied to a surface created in the FEM model space. The software allows for different floor designs and different supporting conditions. The software calculates moments, forces, deflections, and stresses but was found to not be easily coupled to Grasshopper in a parametric way. Again, this means it is not used for the algorithm, but it is used to verify and compare the results of the algorithm to.

The structural analysis software Oasys GSA has a Grasshopper plugin which is in beta version. This allows Grasshopper to perform structural analysis within Grasshopper itself without needing to open GSA. This makes it highly suitable for the algorithm. The downside to GSA is that it is not capable of calculating CLT. In GSA itself it is possible to define a layered composite material, but this does not work with the Grasshopper plugin as of the writing of this thesis. It is however possible to use user-defined orthotropic materials in the GSA plugin. This means that if a CLT floor could be translated to a single material with an equivalent E-modulus to CLT, GSA can calculate the moments, shear forces and deflections accurately.

4.3 Composite method

There are various ways to simplify the mechanical attributes of a CLT floor to single values for each direction as opposed to values for each individual layer. The method chosen for the algorithm is the composite method presented by Blass and Fellmoser in 2004. Using the composite theory it is possible to take the strength and stiffness contribution of each layer into account in a single value that can be used to describe the performance of the floor (Blass & Fellmoser, 2004, p1003-1004). Depending on the number of layers and the E-modulus of the layers it is possible to define the effective E-modulus of the floor in two directions. This method was chosen as it makes it possible to calculate an effective E-modulus regardless of the moment of inertia of the floor. This makes it a suitable method as the custom material in GSA only has an E-modulus input because the moment of inertia is dependent on the geometry of the cross-section. Using equations 1 and 2 the factors k1 and k2 can be determined in which am is the thickness of each layer as illustrated in figure 19 where m is the number of layers. By multiplying the E-modulus of the used timber parallel to the grain

by the factors k1 and k2 the E-modulus in the major and minor direction of the floor can be determined. For example, a 5-layer CLT floor with layers of 30 mm made up of C24 timber is considered. The E modulus C24 parallel to the grain (E0) is 11000 MPa and perpendicular to the grain (E90) 370 MPa. Using the composite theory, it can be determined that k1 is 0.79 and k2 is 0.24. This means that the effective E-modulus of the floor in the major direction is E0 * k1 = 11000 * 0.79 = 8704 MPa and in the minor direction E0 * k2 = 11000 * 0.24 = 2666 MPa. The effective E-modulus in the major direction is lower than that of sawn timber in its major direction (parallel to the grain). This is logical as in CLT not all the wood is running in the major direction so not all the stiffness is "running" in this direction. On the other hand, the other direction of the floor is significantly stiffer than sawn timber is perpendicular to the grain.

As of the writing of this thesis it is not possible to define custom orthotropic materials in Grasshopper GSA. It is however possible to define these materials in a separate GSA file and read this file in Grasshopper. Therefore, a file in GSA was made in which the different CLT composition materials are defined. The composite method was used to create an orthotropic material representing CLT for 5, 7, 9 and 11 layers. For illustration the material properties for 5-layer CLT as defined in GSA using the results of the composite method is shown in table 1. Using these materials, different properties were made for all the varying thicknesses of the CLT. Starting at 5 layers of 20 mm thick each subsequent property increases the thickness of each layer by 5 mm until all layers are 40 mm thick. After this it will add two layers and start increasing the layers again by 5 mm each step. These configurations are all loaded into Grasshopper so the algorithm can pick the correct property (material and thickness) for each calculation. The list of available configurations is shown in table 2.

This process of defining the orthotropic material and the various configured properties using the composite theory and GSA was repeated for the rotated configurations. As the previous chapter on the optimization strategy showed, a 5-layer CLT floor effectively becomes a 3-layer CLT floor after rotating with a thick middle layer (consisting of three layers of timber) and two outer layers. This makes it possible to apply the composite method again to determine the materials and the properties of the rotated CLT as well. This is also loaded in Grasshopper so that the algorithm can pick these rotated properties and assign them to the zones it finds that need to be optimized.

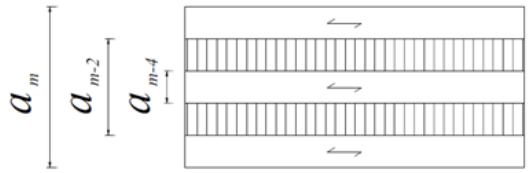

Figure 19: Example of am for m = 5 (Blass et al. 2004, p1003)

$$k_1 = 1 - \left(1 - \frac{E_{90}}{E_0}\right) * \frac{a_{m-2}^3 - a_{m-4}^3 + \cdots \pm a_1^3}{a_m^3}$$ *[Eq. 1 (Blass at al. 2004, p1003)]*

$$k_2 = \frac{E_{90}}{E_0} + \left(1 - \frac{E_{90}}{E_0}\right) * \frac{a_{m-2}^3 - a_{m-4}^3 + \cdots \pm a_1^3}{a_m^3}$$ *[Eq. 2 (Blass at al. 2004, p1003)]*

Table 1: Properties of 5 ply CLT in GSA

Property	Unit	Value
Elastic modulus Ex	[MPa]	8703.92
Elastic modulus Ey	[MPa]	2666.08
Elastic modulus Ez	[MPa]	2666.08
Poisson's ratio vxy		0.4
Poisson's ratio vyz		0.4
Poisson's ratio vzx		0.013
Density ρ	[kg/m³]	420
Thermal expansivity αx	[/°C]	2.8e-06
Thermal expansivity αy	[/°C]	2.8e-06
Thermal expansivity αz	[/°C]	2.8e-06
Shear modulus Gxy	[MPa]	690
Shear modulus Gyz	[MPa]	69
Shear modulus Gzx	[MPa]	690
Damping ratio	[%]	0

Table 2: CLT configurations in GSA

CLT configuration: "number of layers" "layer thickness"	Total thickness
CLT 5 20	100(mm)
CLT 5 25	125(mm)
CLT 5 30	150(mm)
CLT 5 35	175(mm)
CLT 5 40	200(mm)
CLT 7 30	210(mm)
CLT 7 35	245(mm)
CLT 7 40	280(mm)
CLT 9 35	315(mm)
CLT 9 40	360(mm)
CLT 11 35	385(mm)
CLT 11 40	440(mm)

4.4 Stresses

Using the methods elaborated above it is possible to accurately simulate the behavior of a CLT floor in Grasshopper GSA and obtain the moments, shear forces and deflections. The next step is to calculate the bending and shear stresses in both directions from these moments and shear forces. As Grasshopper GSA sees the floor as a single material with orthotropic properties it cannot calculate the layered stress distribution in CLT. This means that separate equations must be used to calculate the stress distribution from the results of Grasshopper GSA. The formulas used in the algorithm are the same formulas used in CLT designer presented by Thiel (2013, p81-94). The equations presented by Thiel (2013, p81-94) can be used to calculate the bending and shear stresses given the bending moments and shear forces. The formulas are adjusted slightly to make distinctions between the stresses in de x and the y direction. This distinction is not made by Thiel (2013, p81-94) as the formulas presented are as they are used in CLT designer which is a one-dimensional calculation tool representing a CLT floor as a beam. Both the bending and the shear stresses are calculated using an effective stiffness factor KCLT that is first calculated. In contrast to the composite method, this KCLT factor incorporates the moment of inertia, area, and eccentricity of each layer. It does not give a single effective E-modulus which means it cannot be used to define an orthotropic material in GSA. The factors KCLT,x and KCLT,Y are determined using equations 3 and 4 below. The bending stresses are then calculated using equations 5 and 6 and the shear stresses using equations 7 and 8

$$K_{CLT,x} = \sum\left(E_{i,x} * I_{i,x}\right) + \sum\left(E_{i,x} * A_{i,x} * e_{i,x}^2\right)$$ [Eq. 3 (adjusted from Thiel, 2013, p81)]

$$K_{CLT,y} = \sum\left(E_{i,y} * I_{i,y}\right) + \sum\left(E_{i,y} * A_{i,y} * e_{i,y}^2\right)$$ [Eq. 4 (adjusted from Thiel, 2013, p81)]

$E_{i,x}$ and $E_{i,y}$	Young's modulus of layer i in x and y direction respectively in MPa
$I_{i,x}$ and $I_{i,y}$	Moment of inertia of layer i in x and y direction respectively in mm4
$A_{i,x}$ and $A_{i,y}$	Area of cross section of layer i in x and y direction respectively in mm2
$e_{i,x}$ and $e_{i,y}$	Distance between center of gravity of layer i and center of gravity of CLT element in x and y direction respectively in mm

$$\sigma_x(z) = \frac{M_x}{K_{CLT,x}} * z * E_x(z)$$ [Eq. 5 (adjusted from Thiel, 2013, p86)]

$$\sigma_y(z) = \frac{M_y}{K_{CLT,y}} * z * E_y(z)$$ [Eq. 6 (adjusted from Thiel, 2013, p86)]

E_x and E_y	Young's modulus in x and y direction respectively in MPa
M_x and M_y	Moment in x and y direction respectively as calculated by GSA in Nmm
$K_{CLT,x}$ and $K_{CLT,y}$	KCLT as calculated using equations 3 and 4
z	Height at which the stress is determined in mm

$$\tau_x(z) = \frac{V_x * \int_{A_{0,x}} E_x(z) * dA_x}{K_{CLT,x} * b(z)}$$ [Eq. 7 (adjusted from Thiel, 2013, p94)]

$$\tau_y(z) = \frac{V_y * \int_{A_{0,y}} E_y(z) * dA_y}{K_{CLT,y} * b(z)}$$ [Eq. 8 (adjusted from Thiel, 2013, p94)]

E_x and E_y	Young's modulus in x and y direction respectively in MPa
V_x and V_y	Shear force in x and y direction respectively as calculated by GSA in N
A_x and A_y	Area of cross section in mm^2
$K_{CLT,x}$ and $K_{CLT,y}$	KCLT as calculated using equations 3 and 4
z	Height at which the stress is determined in mm
b	Width of cross section in mm

4.5 Validating stresses and deformations

Using equations 1 through 8, it is possible to determine the stresses in the floors at different locations in the cross section. This way it is possible to check the stresses in all the zones at all layers to determine for each zone if it should be rotated or not and if the stresses are beyond the strength of the used timber.

To determine if the methods chosen for calculating the stresses and deflections in the optimization algorithm will lead to correct results two simple floors were calculated using three types of software namely CLT designer, Dlubal RFEM with the RF laminate plugin and the methods set up in Grasshopper. Because CLT designer calculates a CLT floor as a wide beam it is only possible to calculate a floor with line supports. For this reason, only line-support floors were considered for this validation. The two floors considered are a 3 by 3-meter and a 3 by 6-meter floor. Both floors have a layup of 5 layers of 30mm thick totaling to 150 mm and are uniformly loaded with 5 kN/m^2. The results of both floors are summarized in tables 3 and 4.

Table 3: Results comparison of 3 by 3-meter floor

3 by 3-meter floor	Max bending stress [MPa]	Max shear stress [MPa]	Max deflection [mm]
CLT designer	1.87	0.06	2.6
RFEM	1.90	0.07	2.4
Grasshopper	1.99	0.08	2.4

Table 4: Results comparison of 3 by 6-meter floor

3 by 6-meter floor	Max bending stress [MPa]	Max shear stress [MPa]	Max deflection [mm]
CLT designer	7.51	0.13	36.02
RFEM	7.55	0.15	35.7
Grasshopper	7.75	0.19	38.08

In both cases, the stresses and deformations calculated in grasshopper are equal or larger than the results of the other software tools. A reason CLT designer can lead to different results is that the Poisson's ratio does not affect the distribution of moments and shear forces throughout the floor as it is performing a beam calculation. In RFEM and Grasshopper it was found that the Poisson's ratio concentrates moments and shear forces along the edge of the floor, leading to higher stresses. In Grasshopper a single Poisson's ratio is assigned to a floor where in RFEM each layer is given Poisson's ratio properties. It is unclear how RFEM determines the overall moment and force distribution throughout the floor given this layered Poisson's ratio, but it can be a reason for the observed differences in results between RFEM and Grasshopper. Another reason that can explain the differences in results is that the stiffness of CLT in Grasshopper calculated using the composite method differs from the stiffness of CLT as determined by RFEM.

In both cases the Grasshopper results will lead to a more conservative approach as they are calculated to be higher than in the other calculation tools. It is expected that using a different method of defining the equivalent stiffness and Poisson's ratio can lead to results closer to those of RFEM and CLT designer. However, it was chosen to accept the results from Grasshopper as the methods used allowed for good integration in the optimization algorithm and the results are deemed accurate enough for the first version of this optimization algorithm.

4.6 Anemone

The final tool that is used for the algorithm is a plugin for Grasshopper called Anemone. Anemone allows the user to loop code in Grasshopper. Natively this is not possible in Grasshopper unless code is directly written in a Python or C# script. Anemone allows the algorithm to loop the GSA calculation and the stress calculations until an optimized result is found. Each iteration it is checked which zones should be rotated and the stresses are calculated. If the stresses or deflections are too high, the thickness of the floor is increased and another iteration of the algorithm is done. This is done until all stress and deflection requirements are reached.

5
Optimization algorithm

Now that the optimization strategy, tools, and methods used in the algorithm are all explained the logic behind the algorithm can fully be explained. This will be done by walking through the script and describing how the logic of each part works. After which an example of a single loop iteration will be elaborated.

5.1 Floor geometry input

The first step in the optimization algorithm is to define the geometric design of the floor. As input for the GSA calculations a surface geometry is required. As this is a generic parameter type it is possible to define this surface in many ways within Grasshopper. The simplest way is to make a rectangular floor by giving a width and a length, but other shapes are possible. As the aim of the optimization is to minimize the amount of timber required it is best to use rectangular floors as much as possible. This is because floors with other shapes will generate more waste during production as planks will have to be cut at an angle making it less likely that the residue of these planks can be used for other floors.

The openings in the floor can be defined by a curve, a surface, a brep or any other geometrical data type. Again, this makes it highly flexible how the openings in the floor can be generated. The geometry representing the opening is subtracted from the surface representing the floor resulting in a large floor surface with openings in it. This surface is passed on to GSA to perform the calculations on. Again, it is possible to define all sorts of openings in the floor, but rectangular openings will lead to the most efficient use of material. Especially if the opening of the floor can be situated with the width of the planks in the floor in mind it is possible to create openings that will require very little parallel sawing of planks in the production process. The design of the floor will impact the amount of timber waste during production, but this is not considered in the optimization algorithm. It is up to the user to realize what kind of floors are suited better for the optimization and how choices in the floor design impact the production procedure. The algorithm will give a layout of planks in the floor as a result which makes it simple to estimate how efficient the production process will become. After running an optimization, it can become clear that an entire row of planks would have to be sawn along its length for example. Based on this, the user could change the input parameters to make the floor fit the plank width better or change the plank width itself. Of course, the design of the floor is governed by the design of the building it will be placed in. This means that sometimes a solution must be accepted where there is a significant amount of timber waste during production. It is however expected that the timber waste during production will always be less than that of conventional CLT.

5.2 GSA: support conditions

After the design of the floor is defined in Grasshopper the surface is passed onto the GSA plugin and meshed. A target mesh size of 100 mm is given for the floors as it was found that this gives a good balance between calculation speed and accuracy. This mesh can be seen in figure 20 for a 3m by 6m floor. If the floor dimensions cannot be exactly divided into 100mm by 100mm squares the grid mesh size is adapted such that it is constant over the entire floor. This means that the squares can become slightly larger or smaller than 100mm but will remain rectangular. If there are openings in the floor the component will automatically switch to triangular mesh elements where necessary to accommodate the geometry of the floor.

After the floor is meshed the supports can be defined. This is done by giving nodes of the meshed floor translational and rotational restraints. The nodes that should be supported can be defined in numerous ways as all sorts of support conditions are possible. As some support conditions are more common than others the script has been set up such that it is simple to define common support conditions. For example, the nodes at the edges of the floor are grouped per edge to quickly define line-supports. When using line supports the nodes at one of the edges are all pinned supported (no translation possible but rotation possible). The nodes in the other edges are consequently only supported in z-direction. This makes it so that the structural scheme of the floor is stable but does not create any unwanted clamping conditions anywhere. Defining point supports is done similarly.

Commonly supported points like the corners of the floor and the midspans of the long edges are already filtered from all the nodes so they can easily be selected. When supporting the nodes directly in the floor shear forces peak unrealistically high at the support points. For example, when a 3m by 6m floor of 5 layers of 30mm thick is supported at its corners and loaded with 5 kN/m2 GSA found the shear forces to peak at 356.2 kN/m at the corners (figure 20).

When not the outer corner nodes of the floor are supported but those nodes one mesh square further inward this peak shear force is already decreased to 110.6 kN/m (figure 21). While this decreases the shear force peak by nearly 70% it is still not a realistic way of supporting a floor.

In reality a floor is not supported at a single node but at a small, distributed area the size of the column connection under the floor. To ensure proper load transfer and rotation capacity a rubber sheet is often put in between the column and the floor. To model this point support condition better some elements have been added to the model (figure 22). From the supported node the 9 closest nodes in the mesh grid are grouped together. These nodes are connected with line elements (dark blue in figure 22) to a steel plate (red in figure 22). The center node of the steel plate is then supported with the correct restraints. The line elements connecting the floor and the steel plates are made of a fictional ductile material (E = 300 MPa) to ensure they do not generate a clamping action at the supported areas of the floor. If these elements would be modelled with a stiffer material like steel the shear forces would still unrealistically peak. Using a ductile elements for these line elements results in a decrease in these shear peaks. On the other hand, a more ductile material results in larger deformations than a stiffer material. After experimentation it was found that a material with a young's modulus of 300 MPa would increase deformations insignificantly while decreasing the shear force peak significantly.

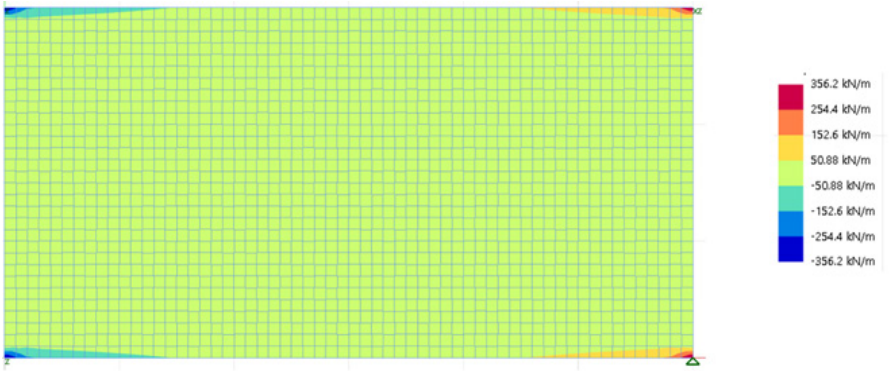

Figure 20: Shear forces in 3-m by 6-m floor supported at outer corners

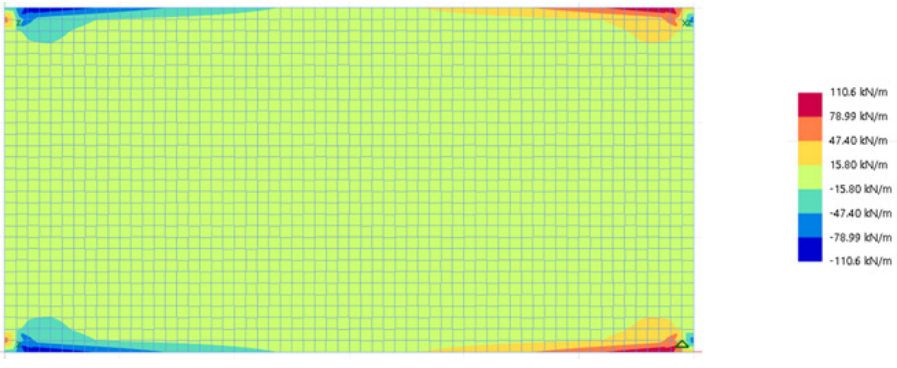

Figure 21: Shear forces in 3-m by 6-m floor supported at one mesh square inward from corners

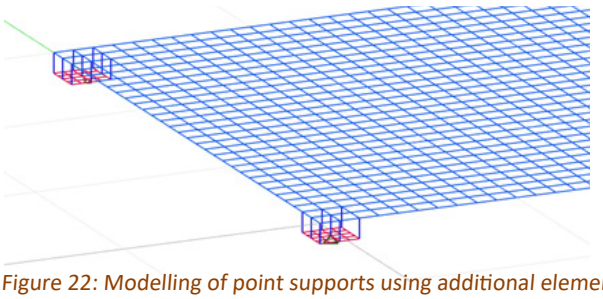

Figure 22: Modelling of point supports using additional elements

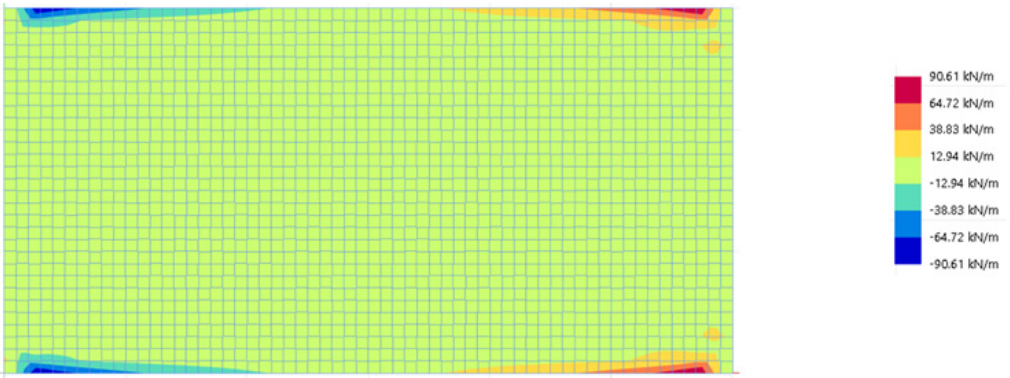

Figure 23: Shear forces in floor supported with additional "rubber" and steel elements at corners

Applying these extra elements to the supports reduced the shear force peak in the floor to 90.6 kN/m (figure 23). The extra elements in the model are not loaded, their self-weight is not taken into account and the stresses in the steel plates and ductile line elements are not taken into consideration. These extra elements purely exist to distribute the forces in the floor more realistically. In the Grasshopper script these elements are automatically added to the model when a point support is defined. For the point supports at least one point must be pinned, another one must be restrained in x and z translation and the other points must only be supported in the z direction. This way, the structural scheme of the floor will always be stable while not unintentionally restricting rotation in the floor creating a clamping effect.

5.3 GSA: load cases/combinations

The optimization algorithm optimizes simultaneously for stresses and deformations so that the resulting floor will fulfill all requirements. According to building code (NEN-EN 1990 in the Netherlands) stresses and deformation should however not be checked under the same loading conditions. The stresses are checked in the ultimate limit state and deformations in the serviceability limit state including creep (long term permanent deformation of timber (NEN, 2013, p26)). In the optimization algorithm the floor is analyzed using a static analysis. This means that the floor only has to be calculated once after which the results can be combined into different load combinations. A single calculation is performed each iteration after which different result combinations are considered for the different checks (stresses and deformations). The stresses are checked under ULS loading conditions according to equation 9, in which G_k is the characteristic value of the permanent loading (self-weight and imposed load) and Q_k the characteristic value of the variable loading. The deformations are simultaneously checked using equation 10 in which Gk and Qk are again the characteristic values of the permanent and variable loading respectively. kdef is the factor taking into account the creep action of timber. The value of kdef is dependent on the climate class in which the floor will be placed (NEN, 2013, p34). The Dutch building code on timber structures does not give kdef values for CLT specifically so the kdef values for laminated timber have been used. The value of φ2 is a reduction factor for the variable loading based on the use type of the building the floor will be located in (e.g. residential, office, store, etc) (NEN, 2011, p61).

In the optimization script the user can define a value for the permanent imposed load and the variable load. The self-weight of the floor is automatically included. The user can also specify the climate class and use class for the floor. This way, the floors are optimized in the script for stresses and deformations simultaneously for the correct loading conditions.

$$ULS\ load = 1.2 * G_k + 1.5 * Q_k \qquad \text{[Eq.9 (Adapted from NEN, 2011)]}$$

$$SLS\ load = G_k(1{,}0 + k_{def}) + Q_k(1 + \varphi_2 k_{def}) \qquad \text{[Eq.10 (Adapted from NEN, 2011)]}$$

5.4 GSA: material/property assignment each iteration

As has been elaborated before the CLT material and floor properties are defined in a separate GSA file that is read by Grasshopper. In this file each lay-up has been defined as an orthotropic material for which the E-moduli in the two horizontal directions has been calculated using the composite method presented by Blass and Fellmoser (2004). Every lay-up is made up of C24 timber. For each floor the shear moduli and Poisson's ratio have been set identical for each layup. In literature various values for the shear moduli for CLT built up of C24 timber have been used ranging from 483 MPa to 690 MPa in the strongest direction G12 (Chiniforush, Valipour, & Ataei, 2021, p14; Haynes, Coleri, & Estaji, 2019, p 164). For the Poisson's ratio values are used in literature ranging from 0.3 to 0.48 in the main direction of the floor v12 (Ahmed & Asiz, 2017, p908; Chiniforush et al., 2021, p14). While it seems that there is no clear consensus on what the correct values are for these attributes for CLT, it is noteworthy that they do significantly influence the results of a calculation or simulation. For illustration table 1 shown in chapter 4.3 is shown again below where all the material properties for the 5-layer CLT lay-up of C24 timber can be found as they have been defined in GSA. The CLT material definitions are custom materials initialized from C24 timber. This means that values like the density are already correct and not changed. The thermal expansivity is also not changed but no temperature study is performed in the optimization algorithm, so the property has no significance for this application. This also holds for the damping ratio.

Table 5: copy of table 1: properties of 5 ply CLT in GSA

Property	**Unit**	**Value**
Elastic modulus Ex	[MPa]	8703.92
Elastic modulus Ey	[MPa]	2666.08
Elastic modulus Ez	[MPa]	2666.08
Poisson's ratio vxy		0.4
Poisson's ratio vyz		0.4
Poisson's ratio vzx		0.013
Density ρ	[kg/m³]	420
Thermal expansivity αx	[/°C]	2.8e-06
Thermal expansivity αy	[/°C]	2.8e-06
Thermal expansivity αz	[/°C]	2.8e-06
Shear modulus Gxy	[MPa]	690
Shear modulus Gyz	[MPa]	69
Shear modulus Gzx	[MPa]	690
Damping ratio	[%]	0

There are 8 custom orthotropic materials defined in GSA: a rotated and a non-rotated equivalent material for 5, 7, 9, and 11 layers. Additionally, 12 2D properties are defined in GSA using these custom materials. These properties include all the possible lay-ups in the optimization algorithm starting with 5 layers of 20 mm and ending with 11 layers of 40 mm. These 12 properties are defined again but then using the rotated version of the orthotropic equivalent material so that they can be applied to the rotated zones in the floors. These 24 properties are loaded into the optimization algorithm where Grasshopper can assign them to the meshed floor.

The first calculation of the algorithm is performed with a fictional isotropic material with the same density and thickness as a CLT floor with 5 layers of 20 mm thick. The criteria for rotating a zone and thus choosing the major direction of the zone is dependent on the direction in which the stress is largest. If a regular CLT floor is used for the first iteration the stress distribution will be affected by the orthotropic property of the floor. When starting with an isotropic floor the stress distribution will fully be governed by the geometry of the floor and the support and loading conditions. This will mean that in the first iteration the required major direction of each zone of the floor will be determined fully based on the original stress distribution. After it is clear what the major direction for each zone should be the first properties are assigned to each zone. The algorithm starts with 5 layers of 20 mm thick. Each iteration 5 mm is added to every layer until all layers are 40 mm thick after which two more layers are added. This is repeated until all stress and deformation checks are satisfied.

To illustrate the effect of starting with a fictitious isotropic material as opposed to starting with a regular 5-layer CLT floor the optimization algorithm is run using both types of floors as a starting position. Figure 24 shows the result when starting with an isotropic material and figure 25 shows the result when starting with a 5-layer CLT floor of which the major direction of all zones is in the x direction. For both cases the floor is 3m by 6m and is point supported at 6 points: at the corners and ad midspan along the long edges. In these figures the planks in the outer layers of the floor are visualized. On the floor itself the moment in x direction is plotted. Starting with an isotropic material leads to more zones running in the y direction. This is logical

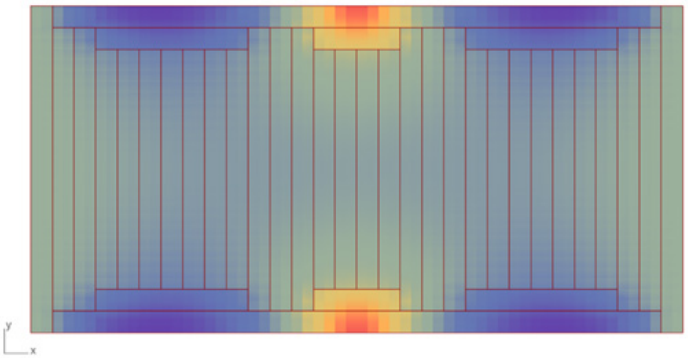

Figure 24: 3m by 6m floor supported at 6 points optimization results starting with isotropic material

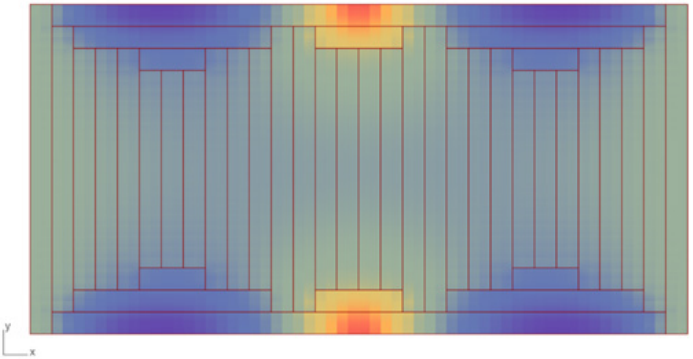

Figure 25: 3m by 6m floor supported at 6 points optimization results starting with orthotropic material

as starting with a floor which has the x direction as its major direction leads to more stresses running in this direction. This means that there are more zones in which the x direction is found to be the major direction. The actual maximum stresses and deformation between the two floors are negligible in this case. Starting with an isotropic floor does however guarantee that for each case it will be certain that the major direction of the floor is solely based on the stress distribution in the floor and not affected by predetermined major and minor directions.

5.5 GSA: sorting results and dividing floor in zones

In the previous sections it was elaborated how the GSA calculation is parametrically set up and how the materials, supports and loads are defined. Within Grasshopper a static GSA calculation is performed in order to obtain the moment, shear force and deflection results of the floor.

The results are given for all nodes in the mesh and at the center of each mesh face. As the optimization zones are based on the plank width, they are 200mm-by-200mm and thus larger than the 100mm-by-100mm target mesh size. Both the optimization zone size and mesh size can be changed but these values have been used for the case studies and presented good results. For each mesh face 5 results are given: one for each of the corners of the face and one for the center of the face. As a first step the average value of these 5 nodes is taken and assigned to the corresponding mesh face. This reduces the effect of unrealistic stress peaks and reduces the amount of data five-fold making the computational time lower. As a next step the optimization zone grid is laid over the floor and thus over the mesh grid. Using the optimization zone grid the mesh faces are grouped by looking which mash face belongs in which optimization zone. This is done by looking at the center of a mesh face. If a mesh face is overlapping in multiple optimization zones, it is assigned to the zone in which its center is located. This grouping is illustrated in figure 26 in which the green crosses are the centers of the mesh faces. After this, each optimization zone is linked to a set of mesh faces. When the optimization zone grid is 200mm-by-200mm and the mesh grid is 100mm-by-100mm there will be exactly 4 mesh faces linked to each optimization zone. Of these linked mesh faces the mesh face with the highest averaged value for the bending moment or shear force will be taken as governing and its values will be assigned to the optimization zone. This way, the optimization zone is always optimized for the largest moments and forces acting within the zone. The bottom part of figure 26 also shows a zoomed in version of a single plank mesh cell with its 4 calculation mesh cells in it and the eventual governing value assigned to a plank mesh cell.

To summarize: there are two sorting steps of the results. The first step is reducing the data to an average result for each mesh face. The second step is finding the highest moment and shear force present in each optimization zone. In the next part of the script the stresses are checked using these maximum values for each optimization zone. This way the amount of data and calculations are reduced while still making sure the floor is optimized for the governing results.

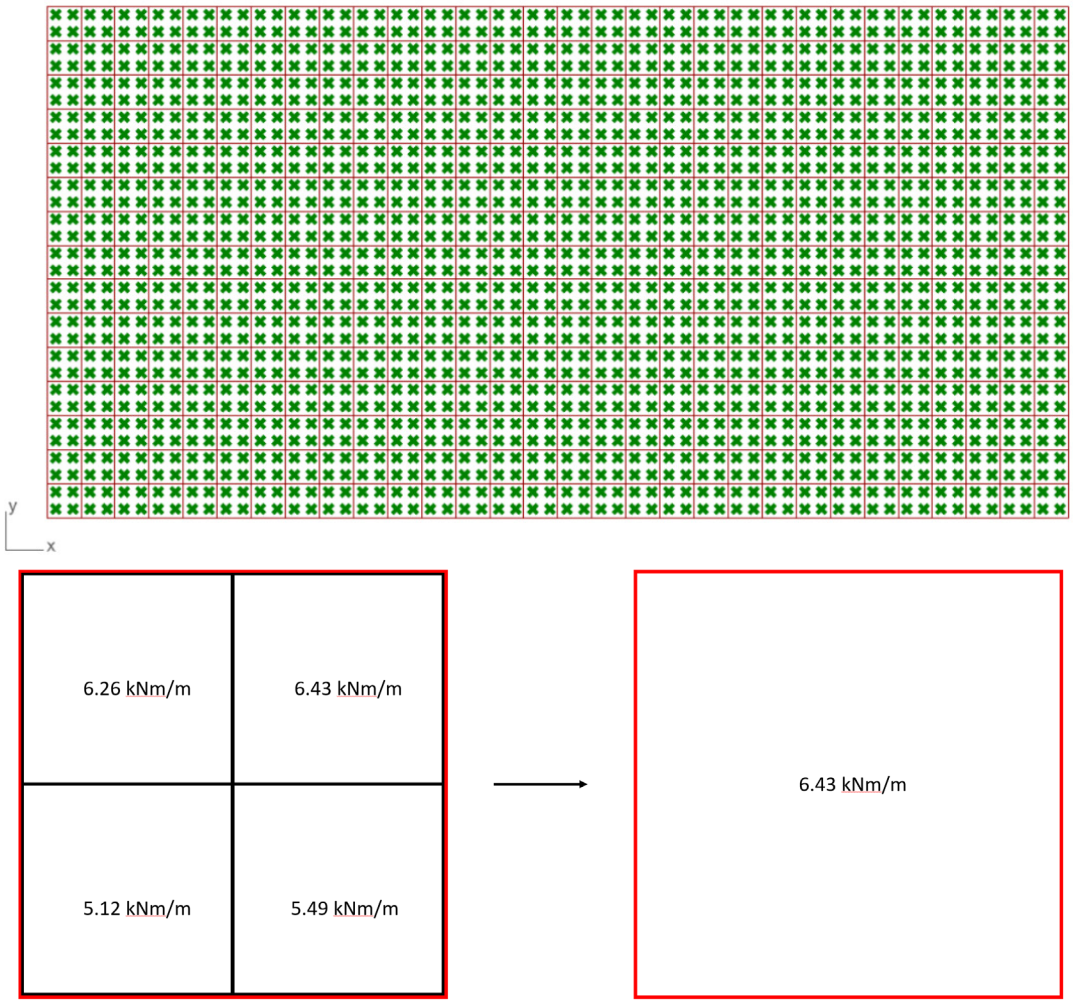

Figure 26: top: 200mm by 200mm optimization zone grid in red. Center of each 100mm-by-100mm mesh face in green Bottom: Assignment of governing value to plank mesh cell

5.6 Stresses

When the results from GSA are sorted and correctly linked to the optimization zones the maximum bending and shear stresses in each zone in both directions are checked. For the optimization algorithm it was chosen to have the non-rotated CLT orientation such that the x-direction is the major direction. By rotating the outer two layers at the top and the bottom of the floor the major direction is changed to the y-direction. In the following section the different stress checks are elaborated. To illustrate this a 3m by 6m floor is used with 5 layers of 30 mm thick and supported at 6 points: the corners and at the midpoints of the long edges. The floor is loaded with an imposed load of 3 kN/m^2 and a variable load of 3.5 kN/m^2. The floor is hypothetically located in an office building and subject to climate class 1. All the stresses are calculated using the equations elaborated in chapter 4.4. By letting the optimization algorithm run without rotating floors it was found that running the major direction parallel to the short edge was the most efficient. Therefore, the floor was oriented such that the short edges are in the x-direction.

5.6.1 Stresses: bending in rotated zones

The first check that is performed is whether the stress in the outer layer in x-direction is smaller than the stress in the second layer from the outer layers in the y-direction (the outermost layer running in the y-direction). If this is the case, it means that the zone should be rotated as the minor direction of the zone is stressed more than the major direction

is. This is visualized in figure 27. When value A is smaller than value B, the zone is rotated. Figure 28 shows the zones where the floor should be rotated overlayed over the displacement plot of the floor. For this floor it was found that the native major x-direction should run parallel to the short edge of the floor. The floor should always be modelled such that the required major direction of the floor runs in the x-direction.

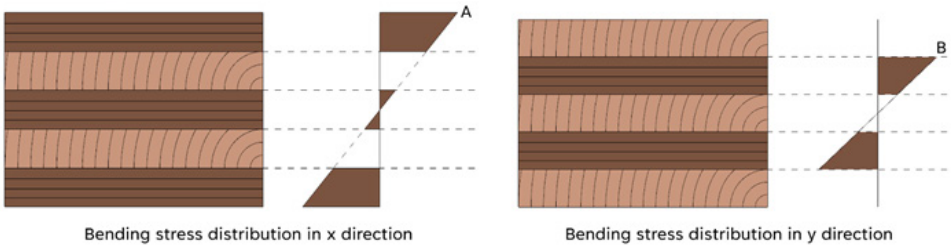

Figure 27: Stresses in major and minor direction of CLT on which rotation criterion is based

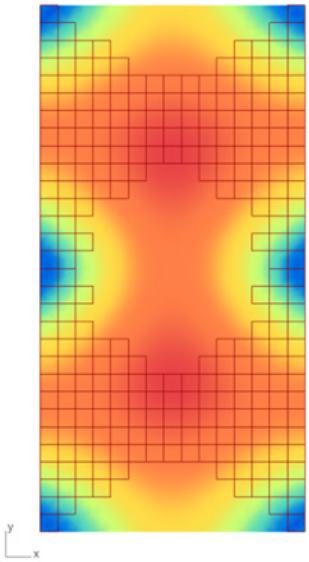

Figure 28: Found rotation zones highlighted over deformation plot of 3m by 6m floor supported at 6 points

When a zone is rotated the y direction becomes the major direction and the lay-up and thereby the stress distribution changes. When this happens two checks are performed. The first check is the bending stress in the outer layer in the y-direction (the new major direction). This bending stress must be below the material strength of the used timber which is C24 for all the cases shown in this research. This means that, given a safety factor of 1.25 the maximum allowable stress is 11.6 MPa as the (NEN, 2016, p10). Figure 29 shows where this stress is most critical and how the cross section looks after rotating. For this case the maximum stress in the y-direction in these critical zones was 11.63 MPa before rotating and 5.75 MPa after rotating. Changing the major direction of the floor leads to a 50% decrease in stress. If these zones would not be rotated the timber would break as the tensile strength parallel to the grain is surpassed at the underside of the floor.

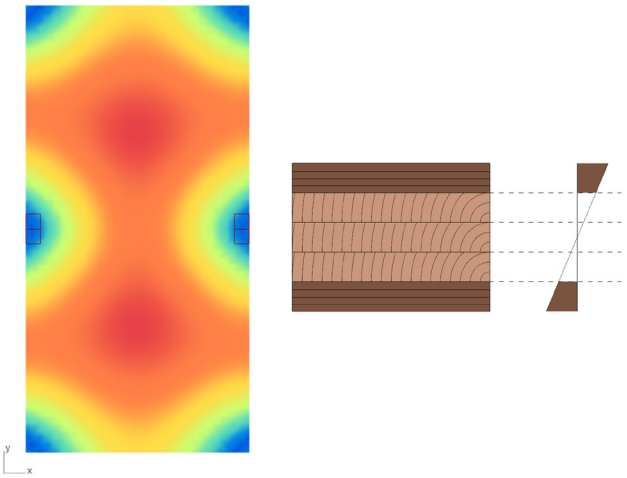

Figure 29: Largest bending stress in major direction of rotated zones occurring in zones indicated by rectangles

Besides checking the new major y-direction, the new minor-x direction is also checked. Rotating a zone and changing the major direction is beneficial for the y-direction but it increases the stress in the x-direction. It is important to check if rotating the zone does not create a problem in the x-direction. Figure 30 shows the areas where the stress in the new minor x-direction is the largest and the cross section in x-direction at these locations. During the use of the optimization algorithm no cases were found where this stress in the new minor x-direction was governing but it will still be checked every iteration.

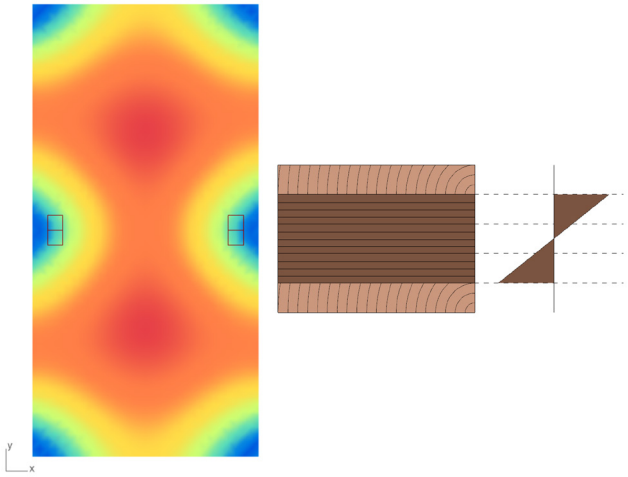

Figure 30: Largest bending stress in minor direction of rotated zones occurring in zones indicated by rectangles

The first two checks that are performed are in the x and y-direction of the rotated zones. The maximum stresses in these zones must be below the strength of the used timber. If they are not, it means the thickness of the floor must be increased so another iteration of the loop is run.

5.6.2 Stresses: bending in non-rotated zones

After it is determined which zones are rotated the stresses in the non-rotated zones are checked. The cross sections at these zones are that of a regular CLT floor. In these zones only the stresses in the x-direction have to be checked. This is because the stresses in the y-direction of the non-rated zones is already checked when deciding which zones should be rotated in the previous step. If the stresses in the x-direction in these zones is too large it means the thickness of the floor must be increased as the x-direction is already the major direction in this case. Figure 31 below shows the location of the most critical non-rotated zones and how the cross section and stress distribution in these zones looks.

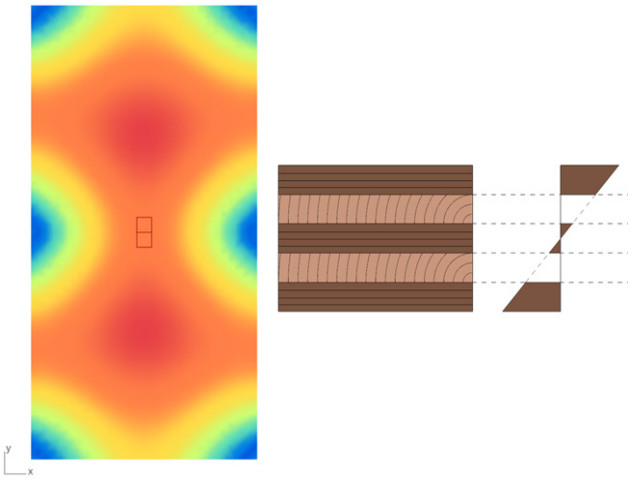

Figure 31: Largest bending stress in major direction of non-rotated zones occurring in zones indicated by rectangles

5.6.3 Stresses: shear in rotated zones

After it is determined which zones should be rotated based on bending the shear forces are checked. Before performing the shear stress checks a check is performed whether the shear stress in the minor y-direction in any of the non-rotated zones is larger than the shear in the x-direction. If this is the case these zones will be added to the rotated zones. During the use of the optimization algorithm no cases were encountered where there were any zones that should rotate based on shear stress and not on bending stress. In all cases the zones that the shear check found were already included in the rotated zones.

Figure 32 shows the location and the cross section of the most critical rotated zones for the shear stress in the new major y-direction. The maximum shear stress occurs at the center of the cross section which is a layer that runs in the x-direction for 5-ply CLT. This means that the shear stress should be checked with the rolling shear strength of the used timber. For all shear stresses the maximum stress in each layer is checked with the corresponding strength of that layer (being rolling shear strength or transverse shear strength). In this example case rotating the zone reduced the maximum rolling shear stress in the center layer from 1.02 MPa to 0.58 MPa. If these zones would not be rotated the design rolling shear strength of 0.8 MPa for C24 timber would be surpassed (NEN, 2016, p10).

Figure 33 shows the location and the cross section of the most critical shear stress in the x direction in the rotated zones. As was the case for bending, rotating a zone causes an increase in stress in the x-direction. It is important to check this stress as well as rotating a zone must not create a problem.

For a 5-layer CLT floor this will likely never happen as the highest shear stresses in the rotated zones are all layers parallel to the grain and thus not dependent on the rolling shear strength of the timber. If the stresses in the rotated zones in the x or y direction are too high, the floor must become thicker, and another iteration of the loop will be run.

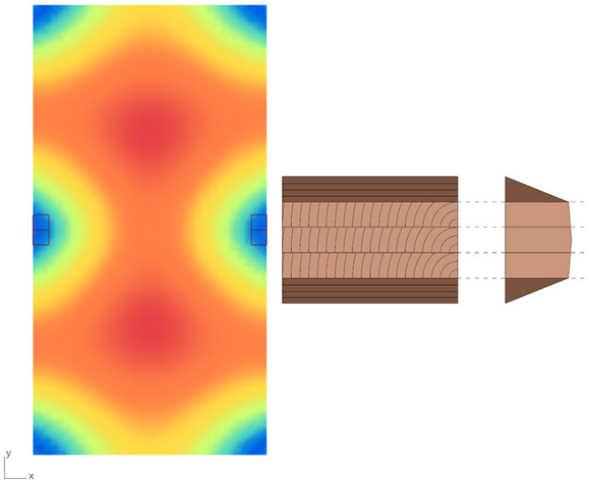

Figure 32: Largest shear stress in major direction of rotated zones occurring in zones indicated by rectangles

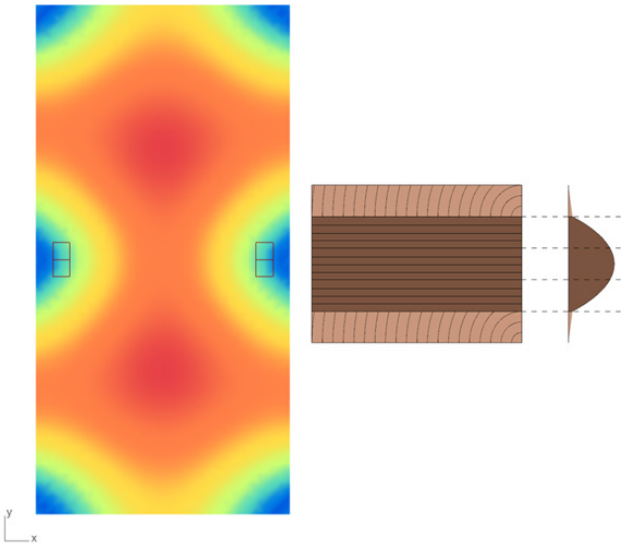

Figure 33 Largest shear stress in minor direction of rotated zones occurring in zones indicated by rectangles

5.6.4 Stresses: shear in non-rotated zones

Similar to bending, the final shear stress check is the shear stress in the x-direction for the non-rotated zones. Again, only the x-direction needs to be checked because if the y-direction stresses would be too high, the zone will be included into the rotated zones. Figure 34 shows the location of the largest shear stresses in the x-direction in the non-rotated zones and the cross section at these areas. Again, the maximum shear stress occurring in each layer is automatically checked with the corresponding shear strength of the direction of the layer (rolling shear strength or regular shear strength).

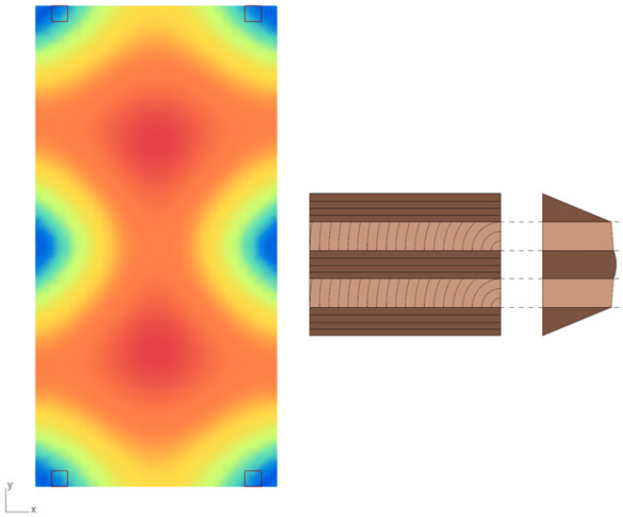

Figure 34: Largest shear stress in major direction of non-rotated zones occurring in zones indicated by rectangles

Multiple stress checks are performed each iteration to make sure the stresses in the floor do not exceed the strength of the floor at any location. This starts by determining which zones should be rotated based on bending. After this the bending stresses in the rotated zones are checked in both directions and the bending stress in the x-direction in the non-rotated zones are checked. After this it the same checks are performed for the shear stresses. If any of these 6 stress checks fails, the thickness of the floor must be increased, and another iteration is run.

5.7 Deflections

The optimization algorithm optimizes floors based on stresses and deflections. The stresses determine which zones should be rotated in order to achieve the optimization. Rotating based on these stresses will also drastically decrease the deflection of the floor. The deflections are not checked per zone but for the whole floor. The displacements are given at the nodes of the calculation mesh.

Lines are automatically drawn between all the support points as shown in figure 35. These lines represent all the span lengths to which the maximum deflections should be checked. From the GSA results the location of the 4 highest deflections are retrieved. By checking the 4 highest values it is ensured that the deflection is checked at different locations in the floor. It is then checked which span line is closest to these points of maximum deflection. This way the maximum deflection points are checked according to the corresponding relevant span direction. The deflection value is divided over the length of the span direction to

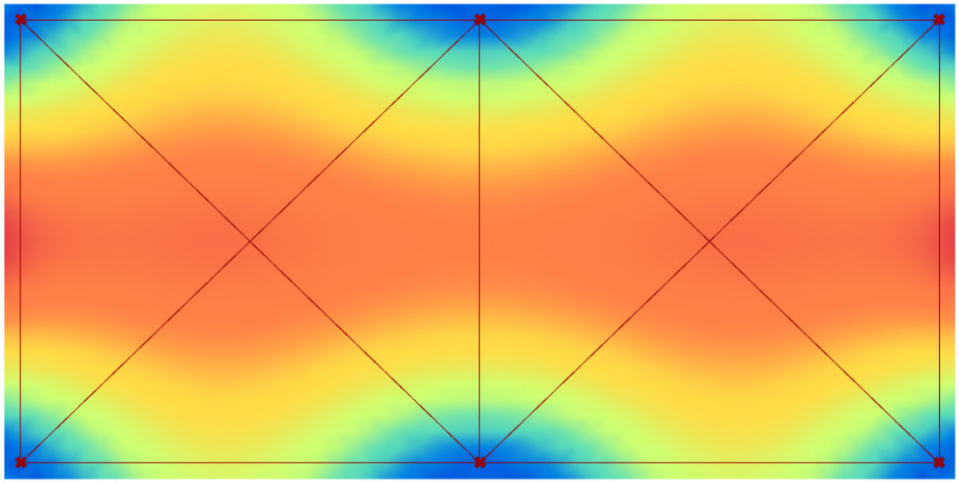

Figure 35: Span directions to which deflections are compared

obtain the slenderness ratio. The minimum ratio is set at 400 meaning that if this ratio is not achieved, the thickness of the floor must be increased, and another iteration of the loop is run. The slenderness ratio can easily be changed in the algorithm.

This method of finding which deflection is closest to which span direction could possibly lead to illogical comparisons. However, during the use of the algorithm in all cases the maximum deflection was checked according to the span length it was supposed to be checked to. To make the optimization tool more versatile this system of defining the maximum deflection criteria can be improved to ensure all relevant deflections are checked correctly.

5.8 Full loop iteration example

To create an overview of the logic of the loop, diagrams have been made that will be elaborated in the following section. Every iteration can be divided into two parts: the first part where the zones that should be rotated are found and the second part where all the stress and deflection checks are performed. Figure 36 shows the steps in this part of the iteration. If a zone should be rotated or not is based on the largest bending stress direction and if there are any zones where the shear stress in the y direction exceeds the strength limit.

After the zones that should be rotated are determined a new GSA calculation is performed where the rotated zones are incorporated in the meshed floor. After this, the stresses and deflections are checked as described earlier. This logic is shown in figure 37

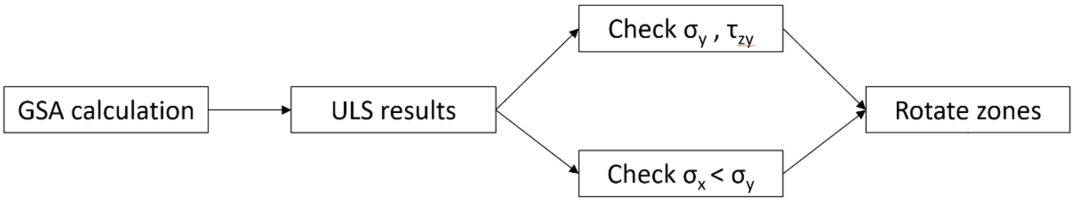

Figure 36: Steps of first half of an iteration

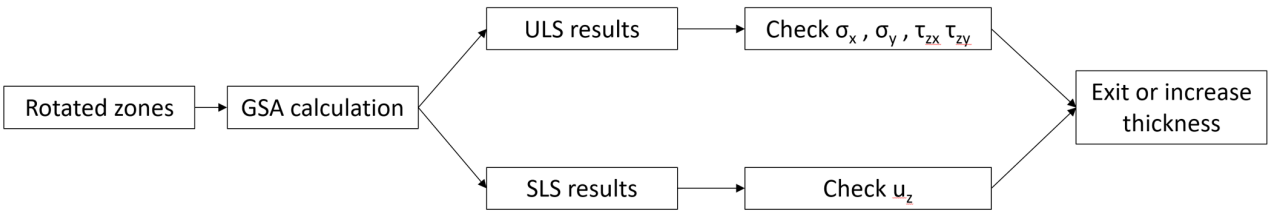

Figure 37: Steps of second half of an iteration

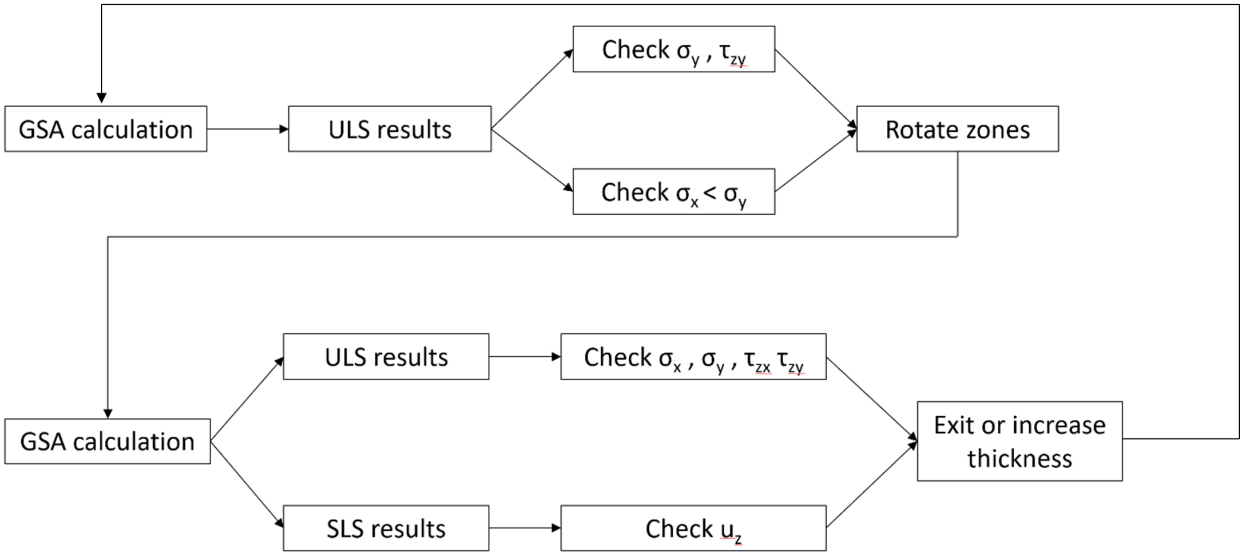

Figure 38: Steps in a single full iteration

Figure 38 shows both parts of a single iteration. As has been elaborated before, the first part of the iteration is mostly relevant during the first iteration where the initial rotation zones are determined using an isotropic floor. After that the first part of the iteration will not change anything to the floors until layers are added to the floor. Adding layers affects the ratio between stiffness in the x and y direction and therefore could lead to more zones needing to be rotated or zones needing to be rotated back to the initial configuration.

The iterative loop is run until the loop exit conditions are met. These conditions are that all stresses and deflection checks must be satisfied. If any of these checks is not satisfied the loop is ran again with two types of data being changed for the next iteration. The first data type is the zones that should be rotated. The loop starts with no rotated zones and after running the first iteration with the isotropic material the zones are found. These zones are then rotated in the following iteration.

The second type of data is which property the floor should get in the next iteration. As elaborated earlier, each iteration the thickness of all layers is increased by 5 mm. This is repeated until all layers are 40 mm thick after which two layers are added. These specific layups for the rotated and non-rotated zones are pre-defined in GSA. At the end of each loop the next layup is selected from the list of all properties and assigned mesh of the floor in the next iteration.

The loop will stop when all the checks are satisfied and remain in the last calculated state. This last calculated state is the minimal thickness with rotated zones for which the floor will satisfy all the stress and deflection checks.

5.9 Plank layout

After the loop is completed and an optimized solution is found the rotated and non-rotated zones are translated to continuous planks. The layout of the planks in the outer layer are visualized. The layers one step in from the outer ones are the exact opposite of the visualized outer layers. The rest of the layers further inward are continuous and do not have rotated planks. This rotation strategy was elaborated in further detail in chapter 3.

6
Case studies

This section will go over three examples of floors optimized using the developed algorithm. The final plank-layout will be shown, and the thickness will be compared to the same floor without rotating. Rotating planks can be turned off in the optimization algorithm which makes it so that the algorithm will keep increasing the thickness of the floor until all checks are satisfied again. This gives a clear indication on how much timber will be saved using the optimization technique

6.1 Case study 1

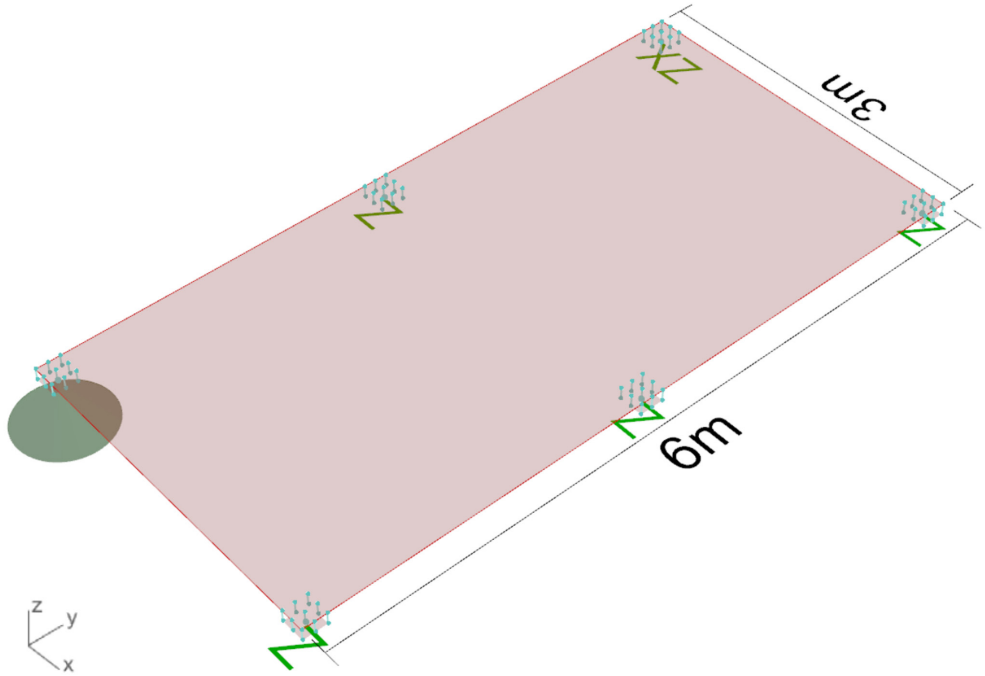

Figure 39: Geometry and support conditions for floor 1

The first floor that is analyzed is the floor that has been used as an example case throughout this report. The floor is 3 by 6 meters and supported at 6 points and has no openings. The floor design is showed in figure 39 where the support conditions for each support point are shown as well. The floor is loaded with a permanent load of 3 kN/m2 and a variable load of 3.5 kN/m2. The floor is located in a commercial store and in climate class 1.

Running the optimization algorithm leads to the plank layout shown in figure 40 where it is overlayed over the moment in the y-direction to illustrate the relation between force distribution and plank direction. The optimization results in a floor consisting of 5 layers of 30 mm thick totaling to a thickness of 150 mm. The governing check was the deflection which determined the total thickness of the floor. If the optimization is run without rotating zones the thickness at which all checks are satisfied is 5 layers of 40 mm thick totaling to 200 mm. For this case the shear stress in y direction was governing. By rotating the zones, the floor can satisfy all stress and deflection checks with 25% less timber. To create a good insight in what the rotation has done for the floor the values of a rotated 150mm thick and a non-rotated 150mm thick floor have been compared in table 6. Because of the rotation in one of the floors the maximum stresses do not always occur in the same places for both floors. The values in table 6 should thus be interpreted to show how the maximum stress value for the entire floor is changed not at a specific location. From this table it can be seen that the maximum stresses in the x-direction increase as this is made the minor direction in the rotated zones. The stresses in the y-direction do however decrease because in these zones the major direction is changed to be in the y-direction. The deflection also significantly decreases due to the rotations.

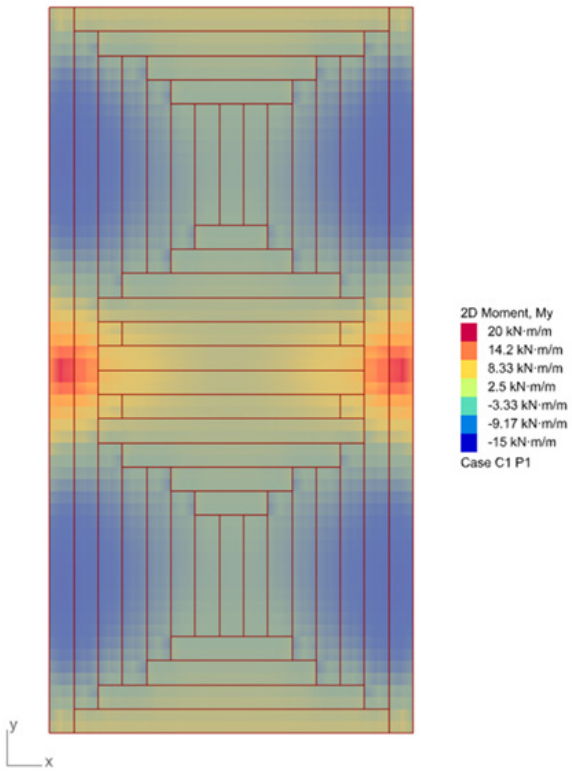

Figure 40: Optimization result of floor 1overlayed on bending moments My

Table 6: Optimization results of floor 1 compared to conventional floor of equal thickness

Value	Rotated 150 mm floor	Non-rotated 150 mm floor	% difference
Bending x [MPa]	6.84	6.13	+11.58
Bending y [MPa]	5.75	10.33	-55.66
Shear x [MPa]	1.07	0.63	+69.84
Shear y [MPa]	0.58	1.03	-56.31
Deflection [mm]	8.47	12.13	-69.83

6.2 Case study 2

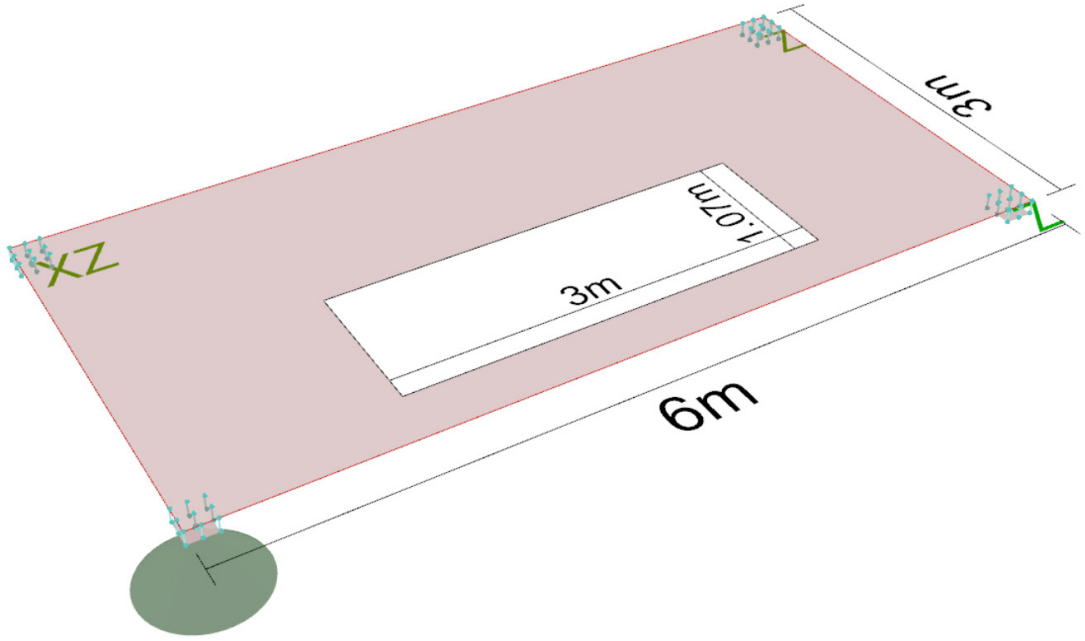

Figure 41: Geometry and support conditions for floor 2

Floor 2 is a 3 by 6-meter floor loaded with a permanent load of 2 kN/m2 and a variable load of 3 kN/m2, located in an office building and in climate class 1. The floor is point supported at the corners and has an opening along one of the long edges for a staircase for example. The floor, its dimensions and supporting conditions are shown in figure 41. The dimensions and the location of the opening have intentionally been chosen such that they do not perfectly fit with the optimization zone grid. This is done to illustrate the script still works for these cases.

Running the optimization leads to a floor of 7 layers of 40 mm thick totaling to 280 mm. The layout of the planks is shown in figure 42. For this floor the governing check was again the deflection. In this case the maximum deflection occurred at the middle of the long span below the opening in the floor. The span distance here is 6 meters which means that the allowable deflection can be 15mm given the slenderness factor of 400. When the optimization algorithm is run without rotating floors the same 7 layers of 40 mm thick are found. This means that rotating zones for this floor does not effectively decrease the thickness of the floor. The maximum deformation of the rotated floor is 12.94 mm while that of the non-rotated floor is 13.23 mm. This shows that rotating the zone does improve the performance of this floor but not significantly. This is not surprising as the critical part of the floor (below the opening) is purely loaded in x-direction. This direction cannot be optimized as it is already the major direction. The solution to optimizing this floor is governed by the required capacity in the x-direction. This direction is the major direction of a regular floor and therefore rotating zones will not significantly increase the performance in this case. Table 7 shows the maximum values for the non-rotated and rotated floor. Here it can be seen that rotating zones decreases all maximum values. Despite this, the floor cannot be reduced in thickness as the rotation does not solve the largest deflection problem significantly enough. This floor shows that for some cases a regular CLT floor cannot be further optimized than it already is using this optimization strategy.

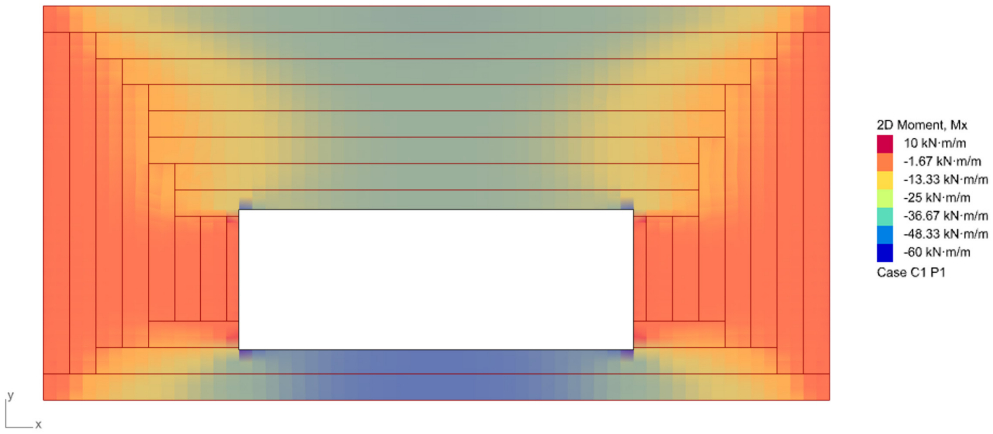

Figure 42: Optimization result of floor 2 overlayed over bending moments Mx

Table 7: Optimization results of floor 2 compared to conventional floor of equal thickness

Value	Rotated 150 mm floor	Non-rotated 150 mm floor	% difference
Bending x [MPa]	5.02	5.04	-0.40
Bending y [MPa]	2.01	2.90	-30,69
Shear x [MPa]	0.50	0.52	-3.85
Shear y [MPa]	0.27	0.37	-27,03
Deflection [mm]	12.94	13.23	-2.19

6.3 Case study 3

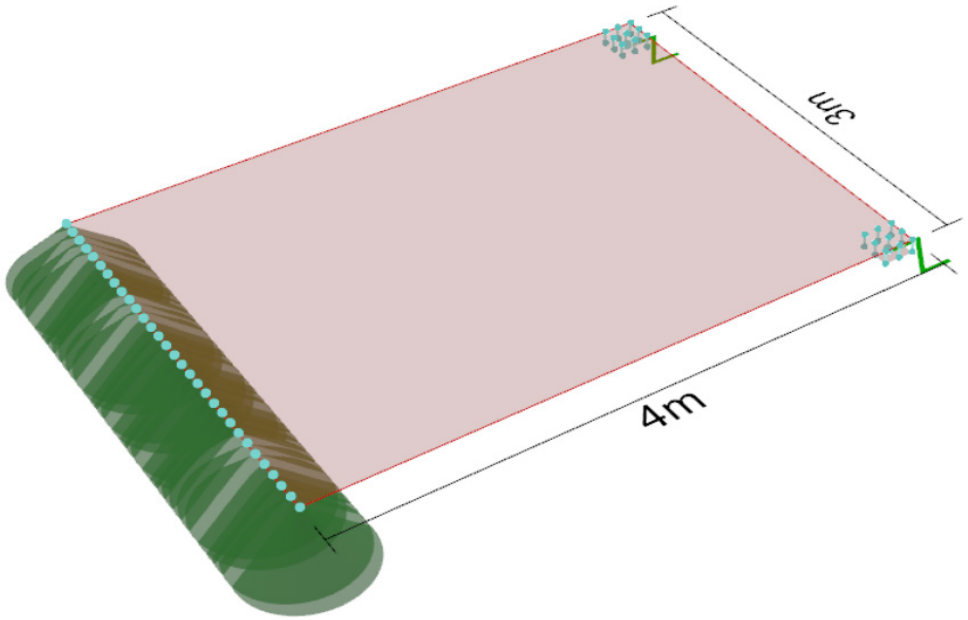

Figure 43: Geometry and support conditions for floor 3

The next floor that was analyzed is a 3 by 4-meter floor supported along its edge on one side and at its two corners at the opposing side. The floor is visualized in figure 43. The floor is loaded with a permanent load of 2 kN/m2 and a variable load of 3 kN/m2. The floor is situated in an office building in climate class 1.

When the optimization is performed a layup of 5 layers of 35 mm thick totaling to 175 mm is found with its plank layout shown in figure 44. When the optimization is run without rotating it was found that all checks were only satisfied when 7 layers of 30 mm thick were used totaling to 210 mm. This means that rotating zones in the floor saves almost 17% timber. Additionally, rotating the zones means the floor can be made with only 5 layers instead of 7. The 17% material saving might be lower than the previously observed 25% but having two less layers in the floor makes the floor faster and cheaper to produce. Less glue and fewer individual planks are required meaning that the 17 % material savings does not paint the whole picture of what is saved in terms of cost and efficiency. For both the rotated and non-rotated floors the governing check was once again the deflection.

This floor clearly illustrates how changing the properties of the floor locally makes the floor behave differently. This is visualized in figures 45 to 47. Figure 45 shows the rotated floor with 5 layers of 35mm overlayed over the deflection with the 4 largest deflection points indicated with red crosses.

The maximum deflection occurs to the right of the center of the floor. This deflection is compared to the main diagonal of the floor where it satisfies the slenderness ratio of 400. When looking at the non-rotated floor of 5 layers of 35 mm in figure 46 the different major direction of the floor results in the largest deflection being located at the short unsupported edge of the floor. This deflection is thus compared to the 3m span of this free short edge. Given that this span is shorter than the main diagonal of the floor, the slenderness ratio of 400 allows for smaller deflections at this location than in the middle of the floor. This causes the floor to fail the deflection requirement. Only when the thickness is increased and there are 7 layers of 30 mm each it becomes evident that the maximum deflection shifts towards the center of the floor. Figure 47 shows the 7 layers of 30 mm unrotated floor that now satisfies the deflection checks. This floor is a clear example of how rotating the zones might not directly reduce the maximum deflection, but it changes the location where the maximum deflection occurs, leading to the deflection checks being satisfied earlier.

Table 8 below compares the values for a rotated floor with 5 layers of 35 mm and a non-rotated floor with 5 layers of 35 mm. These values show that rotating the zones increases all but one of the checked values. This shows that the optimization is working well as it is finding an optimized solution which is not likely when only looking at maximum values.

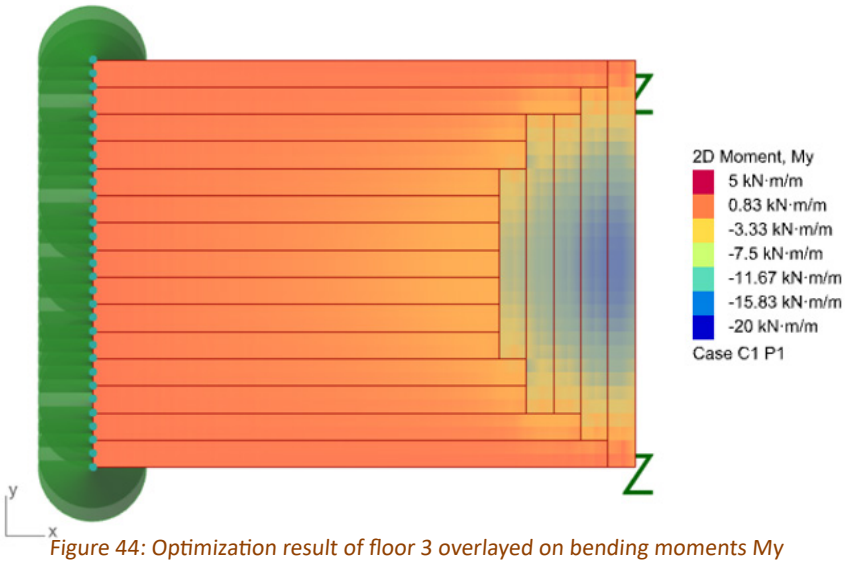

Figure 44: Optimization result of floor 3 overlayed on bending moments My

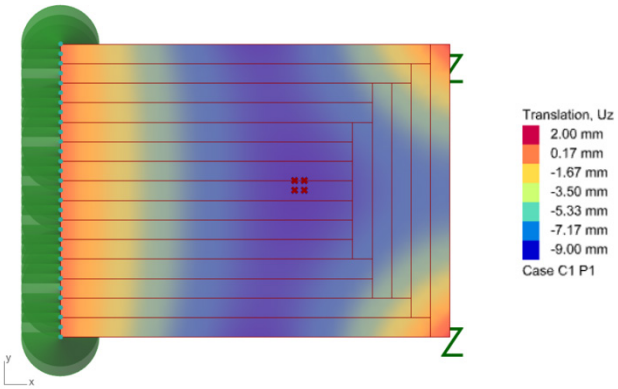

Figure 45: Maximum deflection of optimized floor 3 of 9 mm. Total floor thickness is 175 mm

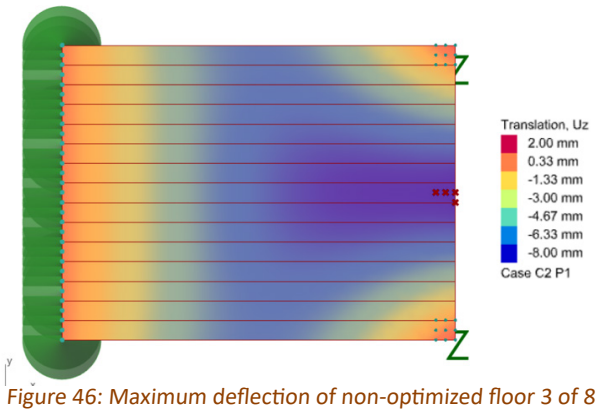

Figure 46: Maximum deflection of non-optimized floor 3 of 8 mm. Total floor thickness is 175mm

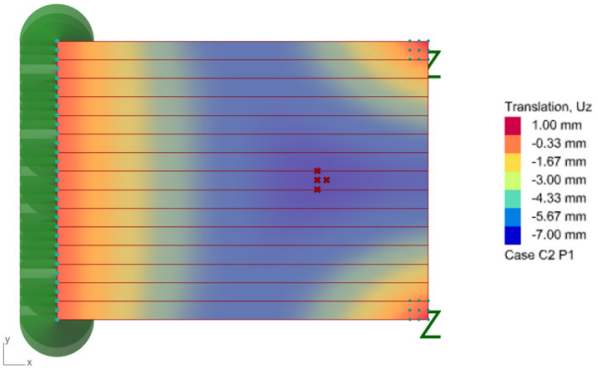

Figure 47: Maximum deflection of 7 mm of non-optimized floor 3 with required thickness (7 layers of 30mm). Total thickness is 210 mm

Table 8: Optimization results of floor 3 compared to conventional floor of equal thickness

Value	Rotated 150 mm floor	Non-rotated 150 mm floor	% difference
Bending x [MPa]	4.58	3.78	+21.16
Bending y [MPa]	3.63	2.06	+76.21
Shear x [MPa]	0.58	0.50	+16
Shear y [MPa]	0.36	0.53	-32,1
Deflection [mm]	8.45 close to floor middle	7.61 at free short edge	+11,03

7

Stresses in rotated CLT

Due to the layered orthotropic nature of CLT the stress distribution in CLT elements follows a step-wise pattern. The way the stresses are distributed throughout a cross section and how this changes when the rotation principle is applied has been elaborated in chapter 3. What is not covered yet is how the stresses are transferred at intersections between rotated and non-rotated zones.

7.1 Bending

the locations where the governing moment in the floor changes in direction rotated and non-rotated zones will meet (see figure 48). At these intersections it must not happen that the strength of the timber perpendicular to the grain is exceeded. The bending moment around these intersections will almost never be the maximum moment for the floor. Additionally, bending stresses in CLT floors are often far below the strength of the timber used because the floors are mostly governed by shear stresses and deformations (see the example case studies). This is all beneficial for these intersection zones as it means the stresses around these zones are somewhat minimalized.

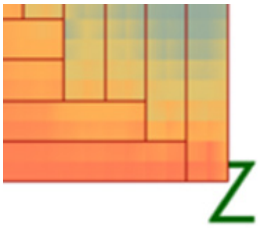

Figure 48: Intersection area between rotated and non-rotated floors

Figure 49 shows how part of the cross section of a floor looks at an intersection area. The stresses must be transferred from the outer layers in the non-rotated zone (left part of figure 49) to the inner three layers in the rotated zone (right part of figure 49). To make this possible it is likely necessary to have a glued bond between the edges of the planks. As elaborated in chapter 2 edge bonding is an existing established concept or CLT. A study has shown that a glued connection between two pieces of timber between which the grain direction is 90o different is fully governed by the strength of timber perpendicular to the grain (Follrich, Hansmann, Teischinger, & Müller, 2007, p88). This means that the stresses in the timber perpendicular to the grain must be controlled. To give an idea of the ratio between the stresses in the timber parallel to the grain and perpendicular to the grain around these intersection areas, a finite element method (FEM) simulation was performed in Abaqus. Creating a full model of a floor including the behavior of the cohesive between all planks is beyond the scope of this research. Instead, a simpler model was made in which a 100% connection between individual planks is assumed. This means that the resulting stress values from the simulation are indicative and possibly not representative of reality. The simulation is performed to see how the stresses flow through the floor at these intersection areas.

A floor of 3 by 3-meters supported at four corners and loaded with 3 kN/m^2 was studied. Running this floor in the optimization algorithm presented the result shown in figure 50. Due to the symmetry in the floor only a quarter of the floor had to modelled in Abaqus. This model was made by creating a single part of 1500mm by 1500mm and 150mm thick. This part was divided into 5 layers of 30mm thick. Each layer was assigned the material attributes of C24 timber as taken from NEN-EN 338 (2016, p10). The point support was created by modelling a 100mm-by-100mm steel plate on which the CLT floor was placed. This plate was supported at a single point in its center. The support was modelled this way to

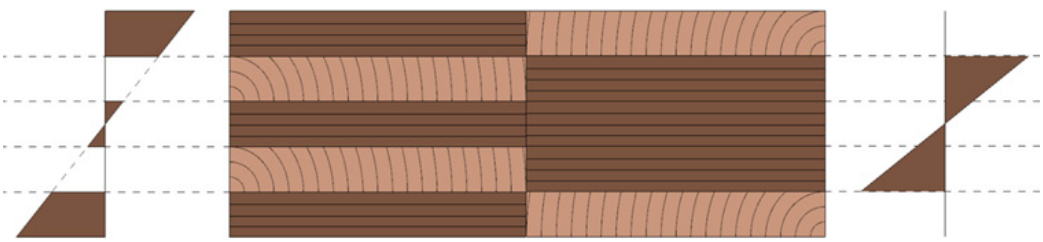

Figure 49: Cross-section of intersection between rotated and non-rotated zone

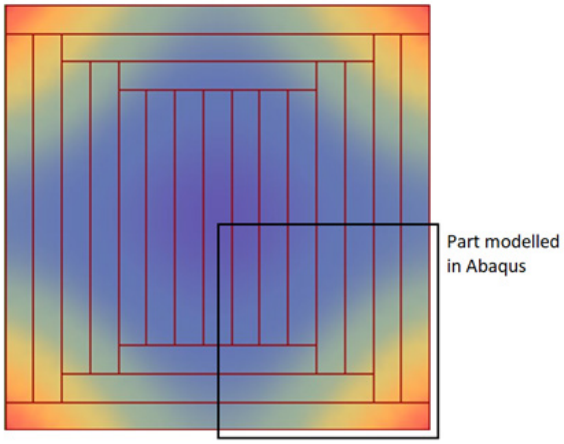

Figure 50: optimization result of 3m by 3m floor supported at corners

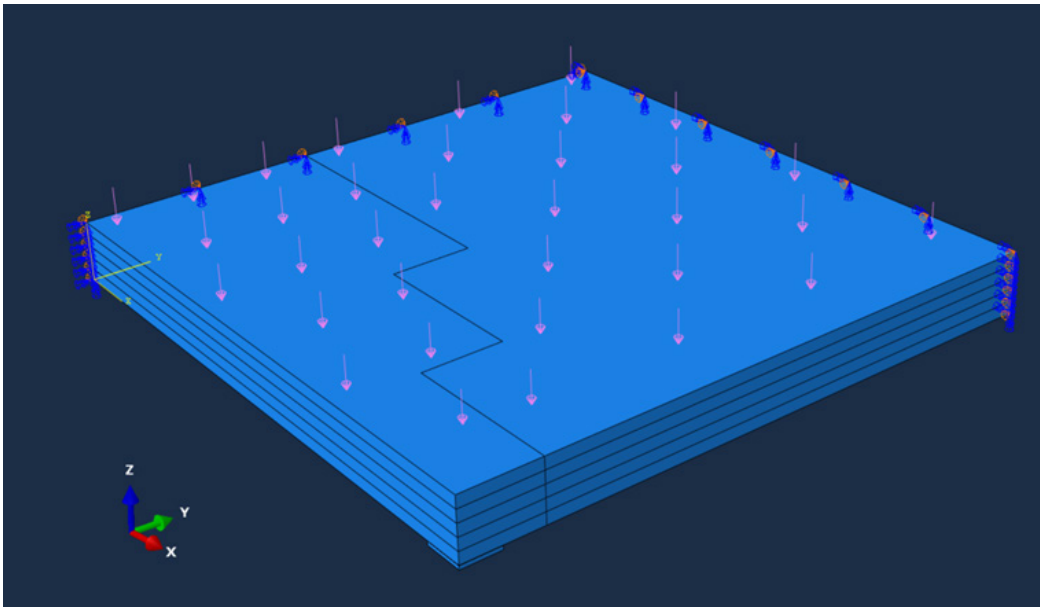

Figure 51: Abaqus model of a quarter of the 3m-by-3m floor. Bottom corner in figure is supported

prevent unrealistic stress concentrations around the support. The floor was loaded by a uniformly distributed load of 5kN/m^2. The Abaqus model is shown in figure 51. The intersection line between the rotated and non-rotated zone is visible. The part of the floor to the right of this line in figure 51 is the rotated zone while that on the left is regular CLT with the x-direction being the major direction.

The results of the FEM simulation can be seen in figure 52 and 53. In figure 52 the stresses parallel to the grain of the timber are plotted and in figure 53 the stresses perpendicular the grain are plotted. The plotted value range has been set such that it is not skewed by the stress results in the steel plate. Figure 52 shows that at both sides of the support the largest stresses are concentrated in the outer layers. This is logical as at both sides of the support the major direction of the CLT was changed so that the outer layers run parallel to the stress direction. From figure 53 it can be seen that the stresses perpendicular the grain increase around the intersection lines between rotated and non-rotated zones. It was observed that the intersection line closest to the support had tension stresses of a magnitude of 0.7 MPa while the stresses located in the intersection zones 200mm away from the support already had tension stresses of 0.3 MPa perpendicular to the grain.

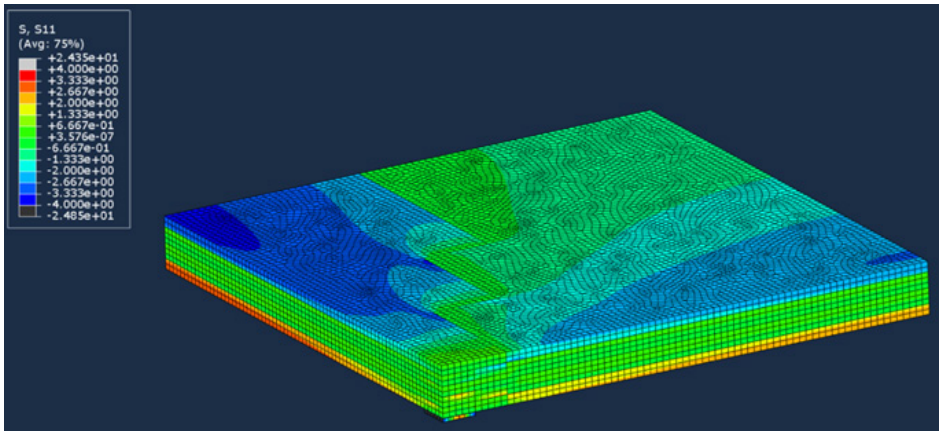

Figure 52: Stresses parallel to the grain

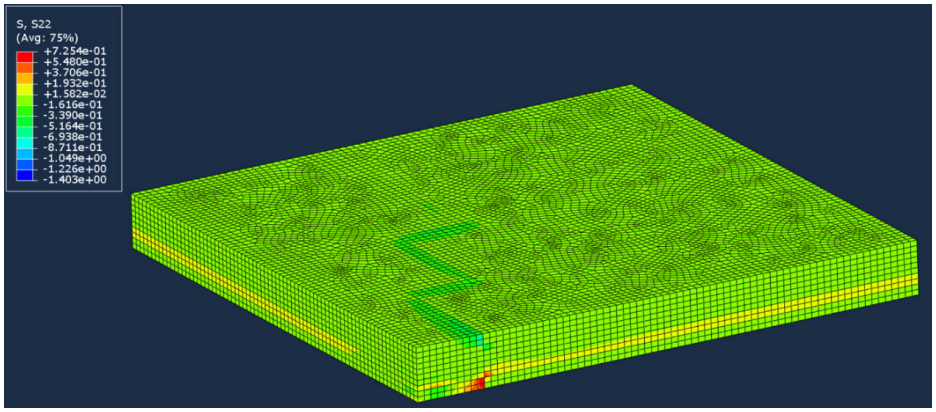

Figure 53: Stresses perpendicular to the grain

7.2 Shear

When looking at the shear stresses there is also an increase in shear stresses around the intersection areas. Figure 54 shows the transverse shear stresses in all layers and figure 55 shows the rolling shear stresses. It can be seen that the transverse shear stresses are mostly concentrated around the support point (bottom corner of the floor in figures) and peak at 2.2 MPa while the design shear strength of C24 timber is 3.2 MPa (NEN, 2013, 2016). When looking at the rolling shear stresses in figure 55 there is a maximum stress of 1.1 MPa. This stress is located directly at the support area at the underside of the floor. When a cut is made in the floor along line AA in figure 55 the results shown in figure 56 are found. Here the shear peak around the support is excluded. The maximum rolling shear stress is still located close to the support but is already reduced to 0.47 MPa. Looking at the stress plot on the floor in figure 56 the intersection zone can clearly be identified showing that there is an increase in stresses around this zone. However, the stresses around this zone peak at only 0.037 MPa, well below the design rolling shear strength of 0.8 MPa for C24 timber (NEN, 2013, 2016, p10). Interestingly, the rolling shear stresses change direction around the intersection zones (values go from negative to positive)

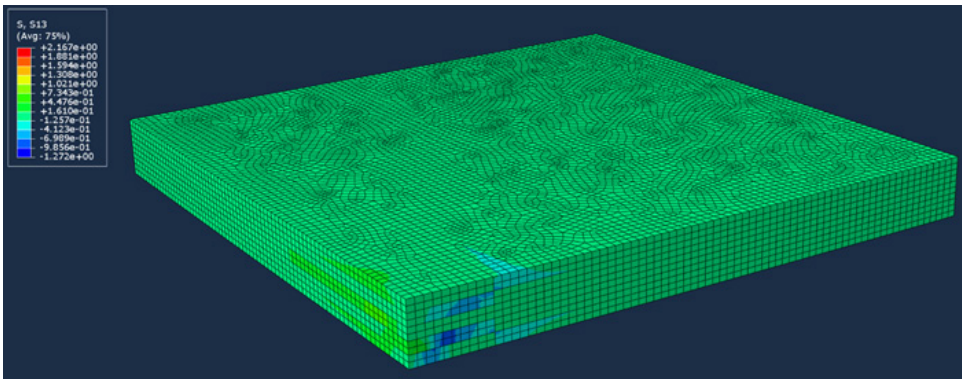

Figure 54: Transverse shear stresses

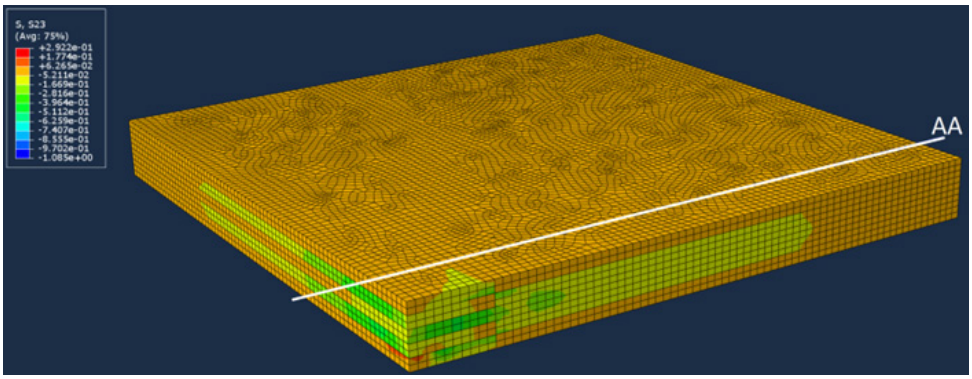

Figure 55: Rolling shear stresses and cutting line

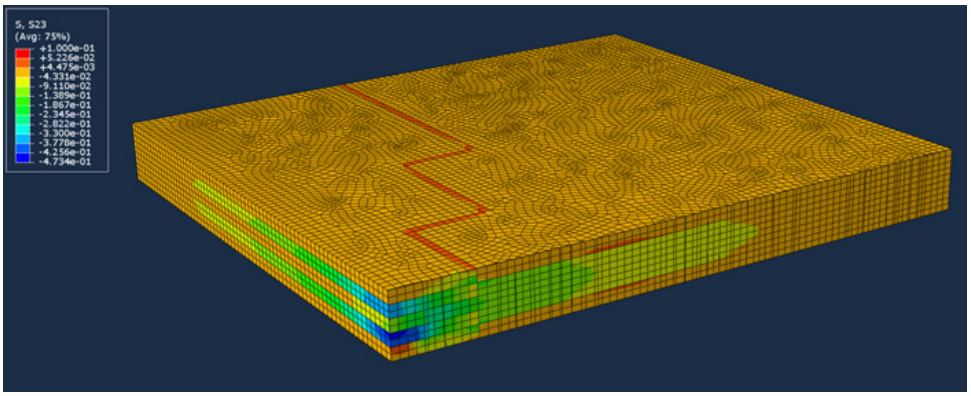

Figure 56: Rolling shear stresses at cutting line

7.3 FEM analyses conclusions

What can be concluded from the Abaqus simulation is that the stresses perpendicular to the grain can become too large, especially close to the supports. The Abaqus simulation also showed that the compression perpendicular to the grain was exceeding the compressive strength of C24. The shear stresses also increase around the support areas and the intersection zones. The rolling shear stress right at the support area was found to be beyond the rolling shear strength of timber but the stresses in the rest of the floor and around the intersection areas are below the strength. While these stresses are indicative it does still show that it is reasonable that stresses exceed the strength of timber around the supports. This is not an uncommon phenomenon for CLT floors that are point supported. Several reinforcement methods exist for CLT around point supports. One such a reinforcement connector is shown in figure 57 of which research has shown that it can increase the capacity of CLT around a point support by more than 80% (Maurer & Maderebner, 2021, p17).

The FEM simulation showed that stress concentrations perpendicular the grain arise around intersection areas in an optimized floor. While the stresses in all the layers are checked during each iteration of the optimization algorithm, the stress concentrations like these cannot be found with the methods used in the optimization. To get a good understanding of how the capacity of the optimized floors is influenced by stress concentrations around the supports and intersection zones more detailed FEM analysis will have to be performed. Ideally some floors would be made full scale and tested in a laboratory to determine the capacity of the optimized floors and their failure behavior. Performing this in-depth FEM analysis and full-scale tests was beyond the scope of this research. If it is concluded that the stresses perpendicular to the grain at intersection areas become too large an adjustment in layup can be made which is shown in figure 58. It is expected that by creating an overlap between the planks in the major direction the stresses will not have to be transferred through the perpendicular planks, eliminating the requirement for edge bonding. The effect of this overlap and how to take it into account in the optimization algorithm is proposed as future research.

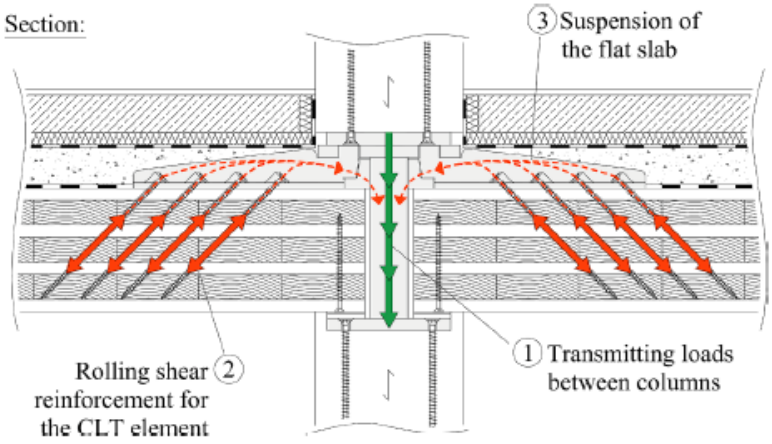

Figure 57: CLT connection and reinforcement system (Maurer & Maderebner, 2021, p2)

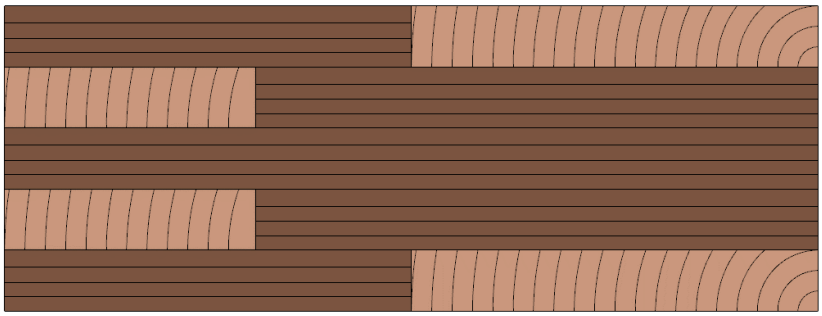

Figure 58: Suggested adaptation to optimization method to improve transfer of stresses

8

Proposed production process

CLT production plants are often streamlined facilities in which multiple machines work together to generate a CLT output of up to 40000 m3 for larger factories (Minda, n.d.). It is important to analyze if production facilities like these could feasibly produce the optimized CLT floors or if brand-new facilities need to be set up in order to reach a profitable production output. In this chapter the adaptations a CLT factory should make in order to produce the optimized floors are explained. This elaboration will be done by going over each step of the production process of CLT as illustrated by Wiegand, Seidel, Mestek, Werther, & Winter (2011, p6-7) in figure 59

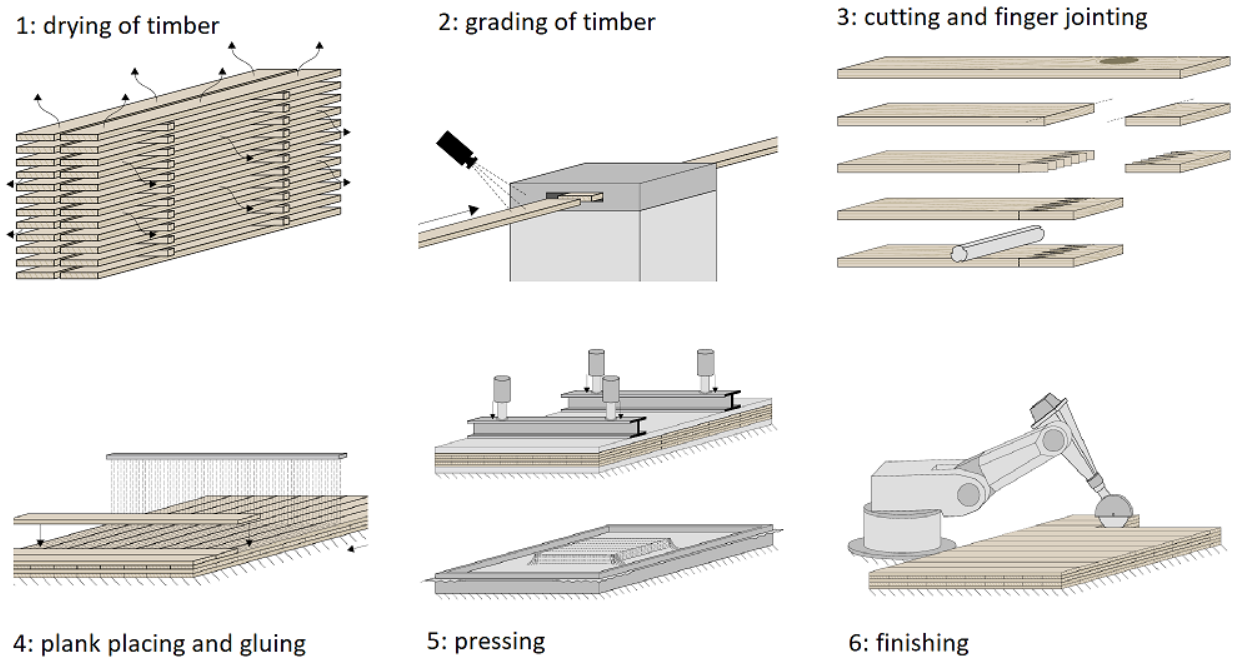

Figure 58: Suggested adaptation to optimization method to improve transfer of stresses

8.1 Production steps 1, 2 and 3

The first three steps of the production of CLT remain unchanged for optimized CLT floors. The optimized CLT floors are made of the same type of timber using the same type of finger jointing as conventional CLT. Where for conventional CLT all finger jointed planks can be of a single length (the width or the length of the panel depending on their layer), the planks for an optimized floor should be cut to their prescribed size in the plank-layout. This means that the output order of the finger jointing and sawing of the planks should be controlled.
It is expected that this extra step will not require any new machinery or robots. It might require a require an adaptation of the conveyor belt system in between step 3 and 4 to keep the required order of the planks.

8.2 Production step 4: plank placing and gluing

Step 4 will undergo the largest change when producing optimized floors. For conventional CLT production a layer of the CLT floor is assembled by placing planks next to each other (possibly with edge bonding). This singular dry (not glued) layer is then picked up using a large vacuum gripper and placed on top of the previous layer on which glue has been applied (Brandner, 2014, p12; WoodSolutions, 2020). For optimized floors the same machinery can be used to create the layers with varying plank orientations. This is because it is still possible to slide the planks in place in a dry layer until a full layer is made. This will require the location where the dry layer is made to have two supply units: one for planks in the x-direction

and one for planks in the y-direction. These supply units need to be able to slide the planks in the correct place which means that they need to be able to precisely move planks in two directions. To illustrate how this feeding order of the planks for a floor works the example floor of 3m by 3m shown in figure 60 is used. In this figure, the order of the planks is indicated by numbering each plank. To further illustrate the order of the planks and how they need to be supplied figures 61 to 63 are made in which planks 6, 7 and 8 of figure 60 are placed.

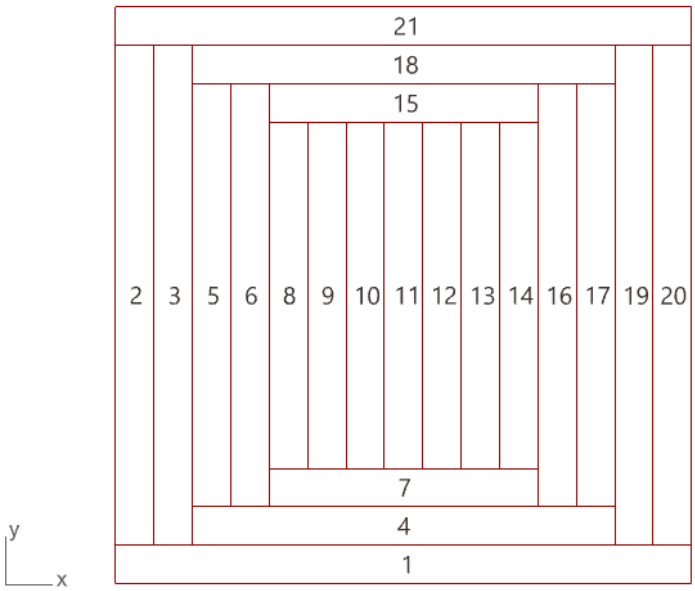

Figure 60: Plank placement order for optimized 3m-by-3m floor

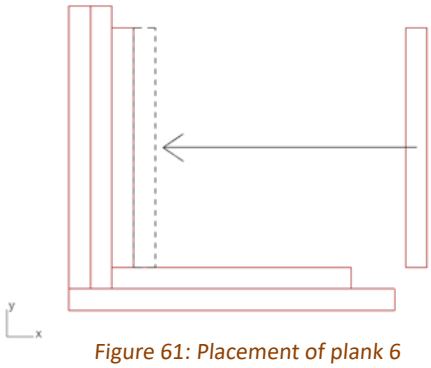

Figure 61: Placement of plank 6

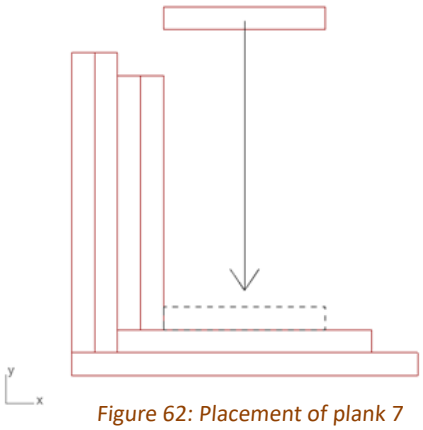

Figure 62: Placement of plank 7

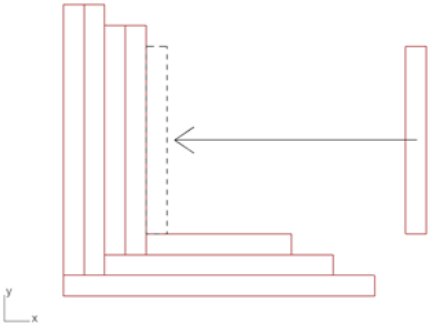

Figure 63: placement of plank 8

For all types of floors there is a logic in which the plank order can be determined whereby each plank can be fed from one of the two supply sides. The first plank will always be the plank that is in the bottom left corner of the floor. In the case of figure 60 this plank 1 is an x-direction plank. The next step is to look at the plank in the same direction that is next to the first placed plank. If this next plank with the same direction is shorter or longer than the first placed plank, it should not be the next plank, but the first y-direction plank should be placed. Hence plank number 2 being the left-most y-direction plank in figure 60. Then the same logic is performed: is the next plank in the y-direction equally long as the plank just placed? In figure 60 this is the case so the next plank will be the next y-direction plank. Then the question is asked again but this time the answer is no. This means that the next plank will be the next x-direction plank which is plank number 4 in figure 60. This logic can be repeated for the full floor to determine the correct plank order.

As the specific sizes and order of planks needs to be determined and followed during production it could also be possible to incorporate large openings in the floor during assembly. For conventional CLT these openings are often cut out after pressing of the panel leading to significant timber waste (Poteschkin, Graf, Krötsch, & Shi, 2019, p102). The planks for optimized floors are already cut to specific length and can thus be placed around an opening. This would however require precise placement of planks by a conveyor/pushing system as not all planks can be pressed together. A solution to this could be to place some sort of mold or negative shape of the opening so that the planks can be placed flush against it. This would however require the mold to be placed midway through the plank placing process and must be taken away again before the vacuum gripper picks up the dry layer. While these steps are possible it will cause interruptions in the production process. Additionally, a system like this will only be feasible if a certain mold can be used multiple times and not for one-off floors. There are already facilities where production with openings is possible. For these facilities the glue application system also needed to be adopted to omit the openings (Brandner, 2014, p17). Further research is required to determine how these types of facilities need to be adapted to facilitate production with openings for optimized floors.

8.3 Production step 5: pressing

After the gluing of an optimized floor as described above the floor can be pressed similarly to regular CLT production. This can be done using mechanical pressing or vacuum pressing. While mechanical pressing can reach a higher pressure than vacuum pressing, it does require a completely even and flat surface of the outer layers of a floor. A vacuum press can allow for variation in thickness or other defects and still maintain an even pressure at all sides (RISE Research Institutes of Sweden, 2019, p17). A vacuum press would thus also be able to press floors with openings in them. The vacuum technique will be able to apply pressure on all surfaces of the CLT, even in the opening.

8.4 Production step 6: finishing

Like the previous step the finishing of CLT floors is no different for optimized floors or conventional floors. A CNC machine can drill/cut the required patterns to facilitate installations in the floor and prepare the structural connections. If the floors are made with openings in them this step would not require cutting the openings and thus significantly reduce timber waste during production.

By analyzing the production of regular CLT and determining what needs to be adapted to manufacture optimized floors it becomes clear that it is possible to manufacture optimized CLT floors using conventional production equipment and techniques. The adaptations to these systems are significant and lay mostly in the ordering and feeding of planks. It is however expected that this can be solved using conventional conveyor belt machinery and would not require the need for expensive or complex robots. Making the dry layers of an optimized floor will take longer than that of a conventional floor. On average CLT floors will need to be hydraulicly pressed 25 to 30 minutes before they can be removed from the pressing machine (WoodSolutions, 2020). An optimized floor might take longer than a conventional floor to be assembled but, if the assembly time can be reduced to 25 minutes or less it would mean the production process is not slowed by the assembly procedure. The process will still be governed by the pressing time.

It would be a significant investment for a CLT factory to create a production line capable of producing optimized floors. However, a CLT factory would not have to invest in new types of machines or robots the industry is not yet familiar with.

9
Discussion

The proposed optimization algorithm can lead to theoretical material savings of up to 25%. The case studies have already highlighted that the optimization technique does not lead to significant material savings for all types of floors. Because the optimization system and algorithm have been set up from scratch, there are still many points of discussion that can influence the practical results of the proposed optimization technique.

9.1 Calculations

The approach of calculating the floors in Grasshopper is somewhat rudimentary: the floors are modelled as solid orthotropic slabs. The layered nature of CLT leads to particular stress and deformation characteristics that might not be fully represented when modeling the floor as a solid orthotropic slab. The formulas used in the algorithm make it possible to calculate the stepwise stress distribution from the moments and shear forces, but these moments and shear forces are calculated using a homogenous floor. The structural calculation models also affect the results of the calculations. As was elaborated in chapter 5.4, there is no clear consensus of what the material properties like the Poisson's ratio of CLT should be. Varying these material properties can have a significant effect on the stress distribution calculated for the floor. This means that it is not fully clear if the calculated results are in line with reality. As was shown in chapter 5.2 some steps were added in the algorithm to reduce unrealistic force and stress concentrations. These methods did reduce the stress concentrations and it was found that these stresses were rarely governing for the optimization. It is however important to mention the effect the modelling approach has on the results. In summary there are many methods and parameters that have been used that together led to expected and acceptable results. It is however important to realize that the calculation and modelling method of the floors can significantly change the calculated values and thereby the outcome of the optimization.

While multiple stress checks are performed in the optimization algorithm not all types of stresses in CLT are calculated. The compressive strength perpendicular to the grain is for example not considered. These stresses can arise around support points and could become governing for a floor. If these stresses are included in the optimization algorithm it can be so that the optimization results will be less significant than they are now. However, as was elaborated in chapter 7.3 there are established CLT reinforcement methods than can significantly increase the capacity of these problematic support areas. The algorithm can be adjusted such that the allowable stresses around supports can be higher given a reinforcement method is applied. For this reason, it is expected that the optimization results will still be significant if these features area added to the algorithm.

9.2 Optimization technique

The optimization technique is based on theoretical stress distribution and a 100% interacting connection between layers and optimization zones. As was shown in the FEM calculation chapter 7 this optimization technique could lead to large stresses perpendicular to the grain around intersections between optimized and non-optimized zones. This calculation is however based on a full connection between all layers and planks. Further FEM calculations and preferably laboratory tests are needed to determine of the proposed optimization technique is viable or not. Chapter 7.3 already proposes a possible adaptation to the optimization technique where there is an overlap between parallel layers to enforce smoother stress transfers. It is however not studied what the effect is of this adaptation.

It is expected that it can be found that the continuous layers in the optimized CLT floor will be stressed significantly when no edge bonding is used as these can become the only layers that can transfer the stresses throughout the entire floor. Especially for 5-ply floors this could become problematic as there is only a single continuous layer. The optimization technique is already not possible for 3-ply CLT but upon further research it could be concluded that it is also not possible in its current state for 5 ply floors as the optimization can be governed by the stresses in the continuous layers.

Additionally, the optimization now works with an equal thickness for all layers. This somewhat limits

the results of the optimization. A stress problem could for example be solved by only increasing the thickness of the outer layers instead of the thickness of all layers. If a varying thickness of layers is implemented, it is expected that the optimization results could be further improved. It must then be studied of it is required to have a constant thickness for each layer throughout the floor or if this thickness can also be varied locally.

9.3 Production

The production process of conventional CLT has been elaborated and studied to determine if the production if optimized CLT is possible. This analysis has been done based on a literature study on the current production process of CLT. This means that the proposed production changes are not supported by figures of estimated cost or production time. While it is shown that the optimized floors can be assembled using conventional factory equipment (conveyor belt systems) future research on the capability of this equipment is required to give an estimation on the feasibility of the production of optimized floors. This needs to be done in combination with CLT factories to take their judgement and expertise into account.

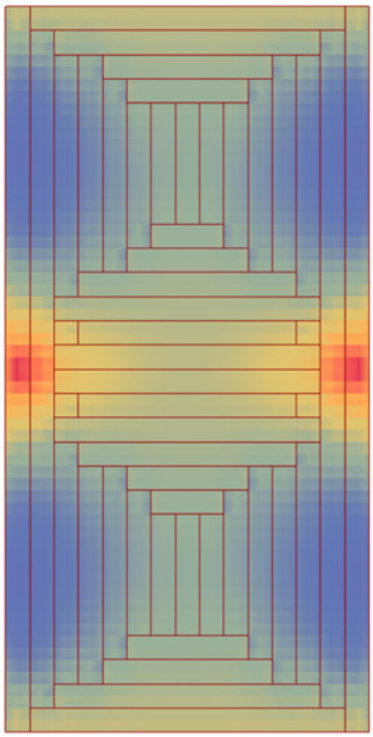

9.4 Reusability

CLT allows for fast pre-fab construction of buildings. In addition, CLT panels could be re-used for multiple structures if their condition is good enough. Because the optimized floors are specifically made for a single loading and support condition, the flexibility in the re-use of these types of floors is significantly reduced. This is a significant downside to the proposed way of creating optimized floors. This downside can however be minimized if the optimization method is applied in combination with modular building systems for example. Modular building systems like that of Dutch company MDLX are based on a standardized structural layouts (MDLX, n.d.). This means that the same type of floors will occur in many of different buildings made with such a modular system. For this scenario an optimized floor can be re-used well as the support and loading conditions in different buildings is often identical.

10
Conclusions

A parametric optimization tool for locally optimizing CLT floors has been presented. The optimization method can lead to theoretical materials savings of 25%. The tool can be used for various types of floors with different geometries, loading conditions and supports. This means that the goal of the research has been achieved. Material savings like these will lead to various effects like lower production costs, faster and easier construction because the elements are lighter, more efficient transport because more elements can be transported at a time and lighter foundations as the weight of the building is reduced.

10.1 Optimization algorithm

By rotating planks in the outer two layers of a CLT floor it is possible to change the behavior of the floor such that the required bending stress, shear stress and deflection requirements are all satisfied with less material. The performed case studies have however shown that there are limitations to the algorithm: the floor of case study 2 could not be optimized using the proposed optimization technique. For the other two case studies the optimization results were significant at 25% and 17% material savings respectively. The 17% material saving for the third case study allows the floor to be made using 5 layers instead of 7 layers of timber which would be required for a conventional CLT floor. This optimization is achieved by looking at the governing bending stress in different zones in the floor. Based on the governing direction it is determined if the major direction of a zone of a floor should be changed. If this is the case the planks in the outer two layers of the floor will be rotated so that the major and minor direction swap. After this rotating of zones, the bending and shear stresses in each layer in each zone are checked alongside the global deflections of the floor. If any of these do not meet the requirements, the thickness of all layers in the floor is increased by 5 mm and the calculations are performed again. This is repeated until all checks are satisfied resulting in an optimized floor. The optimization tool can also be used for conventional CLT to find the minimum required thickness for a floor. This can be done by turning off the rotation function in the algorithm and only optimizing based on the stresses and deflections of the conventional floor.

As the optimization will lead to lighter floors, they are best suited for non-residential applications. The low density of CLT requires additional mass to be placed on the floor to satisfy residential acoustic requirements. For offices or commercial stores, the lighter optimized CLT floors are better suited as it is expected that they will not be governed by their acoustic performance.

10.2 Optimization method

The stress distributions in an optimized floor have been studied using a FEM analysis. From this analysis it can be concluded that the proposed optimization technique can lead to problematic stresses perpendicular to the grain around the intersections between optimized and non-optimized floors, mainly around the support points of a floor. A possible solution to this problem has been supplied but additional research is required to study the behavior of the optimized floors. It is expected that these stress concentrations can be solved using reinforcement methods like additional screws in the CLT panel around the support. This way the optimized floors will not become governed by these local and reinforceable zones in the floor.

10.3 Production

The production of the optimized floors is not yet possible for a conventional CLT factory and would likely require significant investments to make possible. However, it is possible to assemble and produce the optimized floors using the same machinery and tools that are already used in CLT factories. The production lines might have to be adapted to accommodate the production of optimized floors, but no new types of machines or robots are required. It is expected that once adapted, a factory will be able to produce optimized and conventional floors using the same production line. The optimized floors will take longer to assemble as the placing of planks in each layer must be done in a specific order and precisely. The pressing of floors after gluing is however a time-consuming step in the production process taking up to 30 minutes. If the assembly time of optimized floors can be reduced to be faster than the pressing times the output volume of a CLT factory can be similar for optimized floors as for conventional floors.

Because a production line like this would be able to make floors based on a specified plank layout it

becomes possible to incorporate openings in CLT panels during production. This will cause difficulties using hydraulic pressing as the floor could be crushed. Using vacuum pressing or adapted hydraulic pressing (for example by using molds for the openings) these problems can be solved. This would result in significantly less waste during production.

The proposed optimization technique and algorithm are a proof of concept of the capability of locally optimizing CLT floors. The algorithm allows a user to easily find the optimization layout for multiple types of floors. The actual performance and capacity of the optimized floors needs to be studied further. This research is a starting point for various future studies that can lead to significantly reducing material use, costs, and emissions in future construction.

11
Recommendations

The proposed optimization algorithm has been setup from scratch. It is a proof of concept that can form the basis of future research. Many features have not yet been included in this first version. Besides expanding the optimization algorithm, the optimization method also requires more future research. The proposed future research topics are elaborated below.

11.1 FEM and laboratory analysis

The first further research that is suggested concerns testing the proposed optimization method. The proposed method is based on theoretical stress redistribution and FEM analyses have already shown that the stresses can be larger than calculated in the optimization algorithm. These performed FEM analyses assumed a 100% connection between elements and did not include the behavior of adhesives. Incorporating these aspects into FEM analyses and analyzing various optimized floors will lead to a greater understanding of how the stresses are transferred in the optimized floor. In addition, it is suggested that laboratory tests should be performed on optimized floors to study their (failure) behavior. Due to the layered orthotropic nature of CLT it is expected that it is difficult to perform representative experiments on scaled down floors. CLT behavior is highly dependent on the direction of the grain in timber. When scaling the planks in the floor down the grains in the timber will not be scaled down. It is expected that this could lead to different behavior for a scaled down floor than for a full-scale floor. To accurately determine the behavior of an optimized floor it should first be studied what the effect of scaling down CLT for an experiment is before it can be determined how the test specimens should look. If it is the case that these test specimens will need to be full-scale to be representative the next challenge presents itself in making/producing such a floor. As discussed, the optimized floors cannot be made using conventional CLT production methods without some adaptations. It should thus be studied how an optimized floor can be made such that the test specimens will be representative and lead to accurate results.

Another aspect that can only be accurately judged using laboratory tests is how optimized floors behave in shrinkage and swelling. Due to the varying grain direction in a single layer, it is expected that cracks and possible splitting of the timber can occur upon shrinkage in ways that do not occur for conventional CLT.

There are many steps that need to be undertaken before it can be concluded if the proposed optimization technique works or not. However, if the conclusion is that the current method does not work or is not feasible, the algorithm does not have to change significantly. The logic behind the algorithm remains the same: the floors are divided into zones and for each zone it is determined if it should change its major direction. Afterwards the stresses and deflection are calculated to determine if the thickness of the floor should increase. If the optimization method changes it means that changing the major direction is done in a different way. This would result in a different layup but can still be calculated with the equations used in the algorithm. This shows that the algorithm is suitable for a change in optimization method and can adapt to new developments in the technique behind locally optimizing CLT floors.

11.2 Expanding the algorithm

Another topic for further development is improving the capabilities of the algorithm. It has been discussed that there are some stress checks that are not performed in the algorithm like compression perpendicular to the grain. To fully guarantee functionality of the algorithm all forms of stress and deflection checks that can be governing for a floor should be included. In addition to this reinforcement methods can also be included. For example by saying that the stresses around supported zones can be a certain factor higher provided a specified reinforcement technique is used. This way it is expected that the optimization will not be governed by local stress concentrations and still lead to significant material savings

Another feature that could be added is strengthening the initial major direction in zones in the floor. As case study 2 showed, if the behavior in a zone that already has the major direction of the floor is governing, the optimization does not always lead to a thinner floor. The initial major direction

cannot be improved by rotating a zone. A way in which this could be achieved is by locally varying the timber grading that is used. By for example increasing the timber grading of planks in a non-rotated zone from C24 to C30 timber the allowable stresses become higher and the zone becomes stiffer as the E-modulus of C30 is higher than that of C24 (NEN, 2016, p10). Research is required on how varying timber grading in a single CLT floor works. This includes performing research on the stress transfers, displacement patterns, and shrinkage and swelling behavior. If it can be concluded that it is feasible to also vary the strength of timber locally in a floor it is expected that the optimization results will become even more significant.

Another feature that can be researched is removing timber from the floor. Studies have shown that removing timber from a CLT lay-up and essentially creating a hollow core CLT slab can lead to significant material (Mayencourt & Mueller, 2019, p7-8; Moberg & Xiao, 2022, p165-168). Incorporating this feature into the algorithm could lead to locally applying the established optimization technique which in turn could lead to even more significant optimization results.

A final attribute of the algorithm that can further be developed and should be taken into consideration when adding features is the calculation speed. At the current state, the script takes between 30 and 60 seconds to perform a single iteration. For floors that can be less thick this means the optimization can finish quickly but for thicker floors the optimization can take a significant amount of time. It is expected that the optimization algorithm itself can be further optimized to reduce the calculation time making it even more easy to quickly research the optimization possibilities for all sorts of floors.

11.3 Production viability research

A final point of recommended future research is a more detailed study on the production viability of the optimized floors. The performed analysis showed that the production of optimized CLT floors could be possible with industry standard machinery provided some adaptations are made to the production line. More detailed research in collaboration with CLT factories can lead to a more detailed and accurate idea of what these adaptations should be and how much these will cost. Additionally, more detailed research should be performed on the expected assembly time of an optimized floor. While the floors themselves might have lower material costs if the output of the factory is halved, these lower costs will not lead to a larger profit for a factory. The optimized floors can only become feasible to produce if the output volume of an optimized CLT factory can be close to that of a conventional CLT factory.

In conclusion it can be stated that there are many further research topics concerning the optimized CLT floors. This is not unexpected as the optimization method and algorithm have been set up from scratch and work mostly as a proof of concept that locally optimizing CLT can lead to significant material savings.

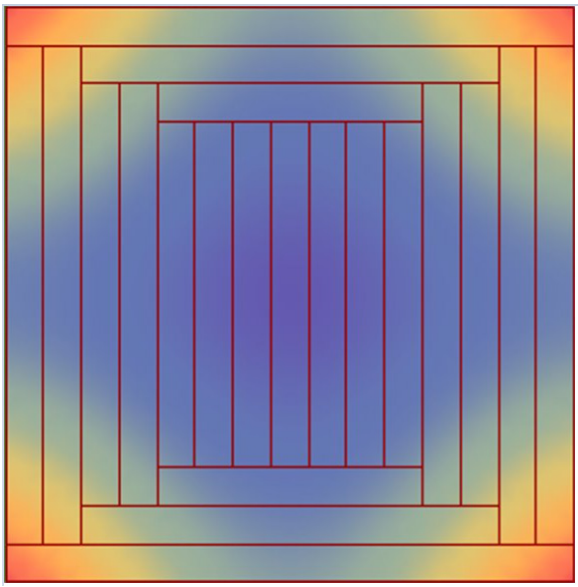

12
References

Ahmed, D., & Asiz, A. (2017). Structural performance of hybrid multistorey buildings with massive timber-based floor elements loaded under extreme lateral loads. *International Journal of Computational Methods and Experimental Measurements*, *5*(6), 905–916. https://doi.org/10.2495/CMEM-V5-N6-905-916

Arup. (n.d.). Haut. Retrieved May 18, 2023, from https://www.arup.com/nl-nl/projects/haut

Blass, H. J., & Fellmoser, P. (2004). Design of solid wood panels with cross layers Influence of shear deformation Design methods for solid wood panels Calculation of solid wood panels with composite theory. *Design of Solid Wood Panels with Cross Layers.*, 604.

Brandner, R. (2014). Production and Technology of Cross Laminated Timber (CLT): A state-of-the-art Report. *Focus Solid Timber Solutions - European Conference on Cross Laminated Timber (CLT)*, (May 2013), 3–36.

Chiniforush, A. A., Valipour, H. R., & Ataei, A. (2021). Timber-timber composite (TTC) connections and beams: An experimental and numerical study. *Construction and Building Materials*, *303*, 124493. https://doi.org/10.1016/j.conbuildmat.2021.124493

Dassault systemes. (n.d.). *Abaqus FEA*. Retrieved from https://www.3ds.com/products-services/simulia/products/abaqus/

Dlubal. (n.d.). *RFEM RF -laminate*. Retrieved from https://www.dlubal.com/en/products/rfem-and-rstab-add-on-modules/others/rf-laminate

Follrich, J., Hansmann, C., Teischinger, A., & Müller, U. (2007). Tensile strength of softwood butt end joints. Part 2: Improvement of bond strength by a hydroxymethylated resorcinol primer. *Wood Material Science and Engineering*, *2*(2), 90–95. https://doi.org/10.1080/17480270701850473

FP innovations. (2020). *The Canadian CLT handbook*.

Grasshopper3d. (n.d.). *Grasshopper*. Retrieved from https://www.grasshopper3d.com/

HAUT Amsterdam. (2022). HAUT. Retrieved May 18, 2023, from https://hautamsterdam.nl/nl/

Haynes, M., Coleri, E., & Estaji, M. (2019). Selection of the most effective pavement surfacing strategy for the Glenwood cross laminated timber parking garage. *Construction and Building Materials*, *226*, 162–172. https://doi.org/10.1016/j.conbuildmat.2019.07.220

Holz.bau. (n.d.). *CLT designer*. Retrieved from https://www.cltdesigner.at/en/

IEA. (2019). Global Status Report for Buildings and Construction 2019. Retrieved January 20, 2021, from https://www.iea.org/reports/global-status-report-for-buildings-and-construction-2019

Liu, Y., Guo, H., Sun, C., & Chang, W. S. (2016). Assessing cross laminated timber (CLT) as an alternative material for mid-rise residential buildings in cold regions in China-A life-cycle assessment approach. *Sustainability (Switzerland)*, *8*(10). https://doi.org/10.3390/su8101047

Mateusz, Z. (2015). *Anemone GH plugin*. Retrieved from https://www.food4rhino.com/en/app/anemone

Maurer, B., & Maderebner, R. (2021). Cross Laminated Timber under Concentrated Compression Loads - Methods of Reinforcement. *Engineering Structures*, *245*(May), 112534. https://doi.org/10.1016/j.engstruct.2021.112534

Mayencourt, P., & Mueller, C. (2019). Structural Optimization of Cross-laminated Timber Panels in One-way Bending. *Structures*, *18*, 48–59. https://doi.org/10.1016/j.istruc.2018.12.009

MDLX. (n.d.). MDLX modular building system. Retrieved May 20, 2023, from https://www.mdlx.nl/

Mela, A. (2023). Why Asumma designs and builds homes from cross-laminated timber (CLT). Retrieved May 18, 2023, from Helsinki Design weekly website: https://helsinkidesignweek.com/2023/01/10/asumma-suunnittelee-ja-rakentaa-laadukkaita-puutaloja-cltsta/?lang=en

Minda. (n.d.). Complete CLT production. Retrieved May 18, 2023, from https://www.minda.com/en/solid-wood-industry/clt-plants

Moberg, A., & Xiao, L. (2022). *Next Generation CLT*.

Mohd Yusof, N., Md Tahir, P., Lee, S. H., Khan, M. A., & Mohammad Suffian James, R. (2019). Mechanical and physical properties of Cross-Laminated Timber made from Acacia mangium wood as function of adhesive types. *Journal of Wood Science*, *65*(1). https://doi.org/10.1186/s10086-019-1799-z

NEN. (2011). *NEN-EN 1990 including Dutch national annex: Basis of Structural Design*.

NEN. (2013). *NEN-EN 1995-1-1 including Dutch national annex: Design of timber structures*.

NEN. (2016). *NEN-EN 338:2016 en Hout voor constructieve toepassingen*.

Oasys software. (n.d.-a). *GSA*. Retrieved from https://www.oasys-software.com/products/gsa/

Oasys software. (n.d.-b). *GSA grasshopper plugin*. Retrieved from https://www.food4rhino.com/en/app/gsa

Penfield, P., Germain, R., Smith, W. B., & Stehman, S. V. (2022). ASSESSING THE ADOPTION OF CROSS LAMINATED TIMBER BY ARCHITECTS AND STRUCTURAL ENGINEERS WITHIN THE UNITED STATES. *Journal of Green Building*, *17*(1), 127–147. https://doi.org/10.3992/jgb.17.1.127

Pereira, M. C. de M., & Calil Junior, C. (2019). Strength and Stiffness of Cross Laminated Timber (CLT) panels produced with Pinus and Eucalyptus: experimental and analytical comparisons. *Matéria (Rio de Janeiro)*, *24*(4). https://doi.org/10.1590/s1517-707620190004.0844

Poteschkin, V., Graf, J., Krötsch, S., & Shi, W. (2019). Recycling of Cross-Laminated Timber Production Waste. *Research Culture in Architecture*, 101–112. https://doi.org/10.1515/9783035620238-010

Püssa, M., & Kers, J. (2017). *The effect of edge bonding to the properties of cross laminated timber*. Tallinn university of technology.

Rhino3d. (n.d.). *Rhino*. Retrieved from https://www.rhino3d.com/

RISE Research Institutes of Sweden. (2019). The swedish CLT Handbook. *Swedish Wood*, 16-17;

Sustersic, I. (2016). Less is more – optimized ribbed CLTs – the future Moins est plus – CLT cintré optimisé – l ' avenir. *22. Internationales Holzbau-Forum IHF 2016*, 1–9.

Thiel, A. (2013). ULS and SLS design of CLT and its implementation in the CLTdesigner. *Focus Solid Timber Solutions European Conference on Cross Laminated Timber (CLT)*, (May), 77–102.

Wallner-Novak, M., Koppelhuber, J., & Pock, K. (2014). *Cross-Laminated Timber Structural Design- Basic design and engineering principles according to Eurocode*. Retrieved from http://www.binderholz.com/fileadmin/PDF/Basisprodukte/Brettsperrholz_BBS/201411_proHolz_Cross-Laminated_Timber_Structural_Design.pdf

Walsh, N. P. (2018). World's Largest CLT Building Provides a Model for High Density Urban Housing. Retrieved May 18, 2023, from Arch Daily website: https://www.archdaily.com/903839/worlds-largest-clt-building-provides-a-model-for-high-density-urban-housing

Wiegand, T., Seidel, A., Mestek, P., Werther, N., & Winter, S. (2011). *Building with cross laminated timber*. 35.

WoodSolutions. (2020). *How It's Made: Cross Laminated Timber (CLT)*. Retrieved from https://www.youtube.com/watch?v=rK49UjDivWM

List of figures and tables

Appendix

Overview of Grasshopper script

In this appendix the optimization script is shown, and the function of each part is elaborated. First an overview of the entire script is given in which the script is divided into 5 main groups of code. It is also indicated that parts B, C and D are part of the iterative loop. Below this overview each of the 5 parts of the script is shown and an elaboration in its function is given.

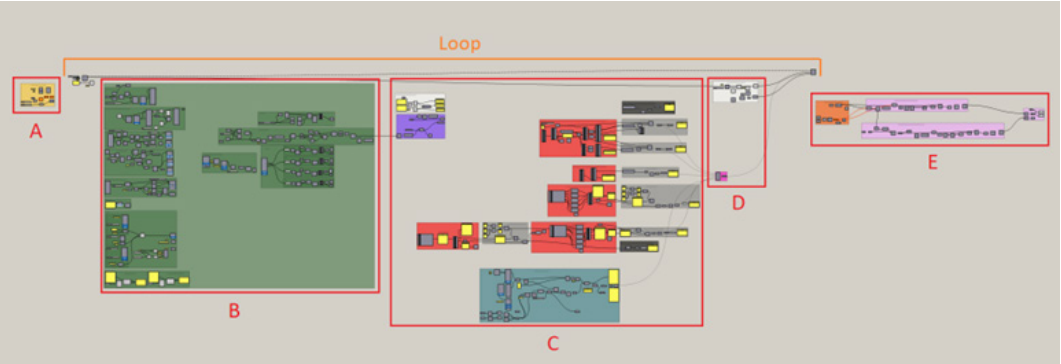

Figure A.1: full script overview

Part A: geometrical input

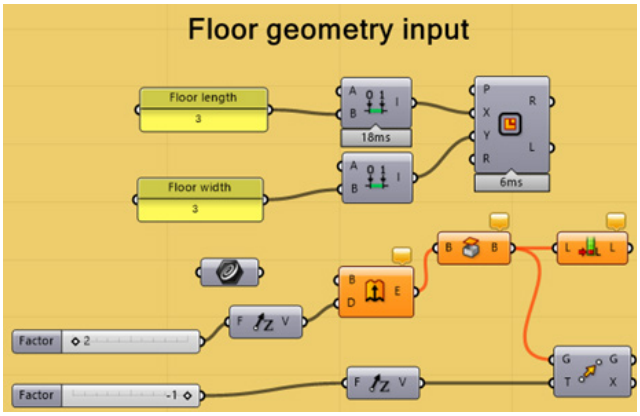

Figure A.2: Script part A

The first part of the script is de definition of the shape of the floor and the openings in the floor. In this case, the floor is 3m by 3m. There are no openings in this floor hence the orange error bubbles. These errors indicate that there is no data running through these components which is correct as there is no opening in this floor.

Part B: GSA calculation

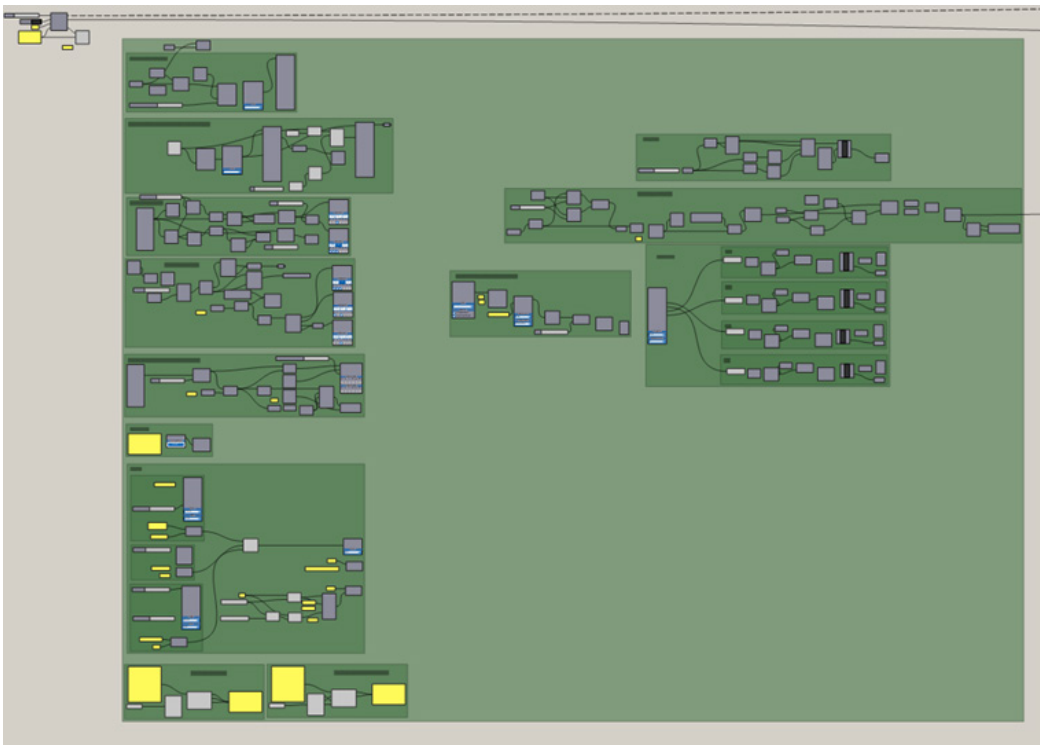

Figure A.3: Script part B

The GSA calculation is set-up and performed in part B of the script. The groups on the left of part B are the set-up of the calculation and include the conversion from floor surface to GSA mesh, the properties of the mesh, the support conditions, the loading conditions and the analysis and combination cases for the calculation. These inputs are fed into the group in the middle of part B where the calculation is performed. The code after this is sorting the results such that each mesh face result in linked to the plank mesh. This is done for the moment in x and y direction and the shear force in x and y direction. At the top left of the figure above the start of the iterative loop can be seen. The looped data is fed from these components into the GSA calculation set-up.

Part C: stress calculations and checks

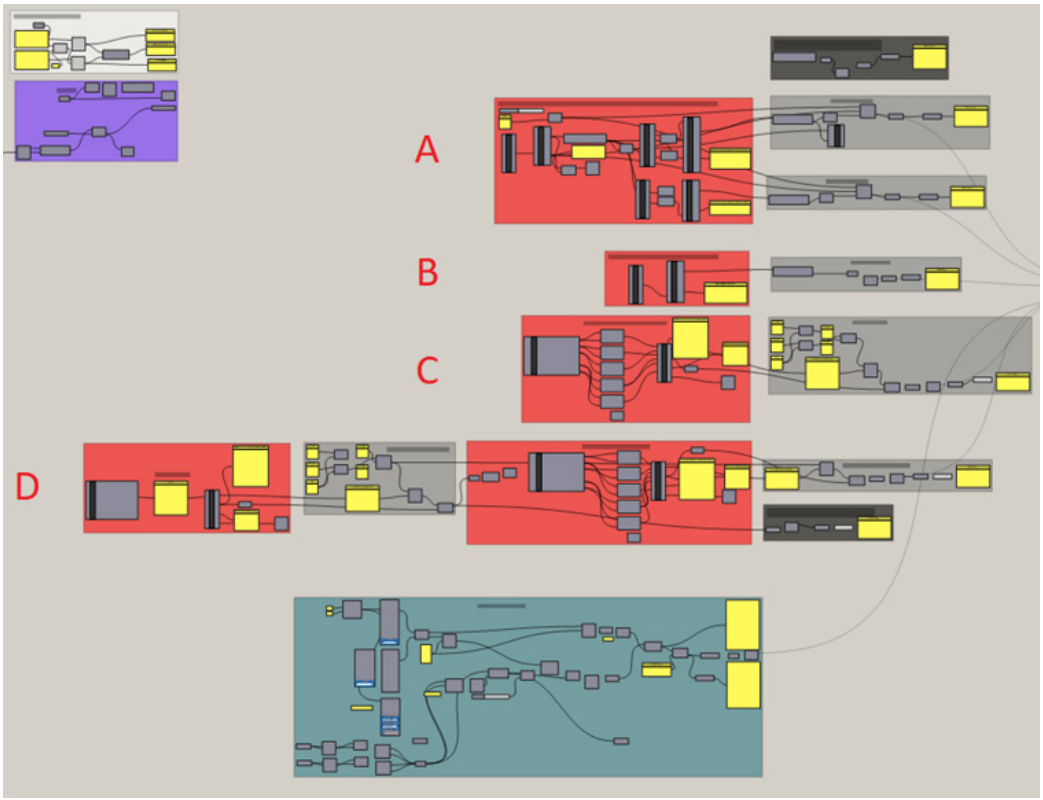

Figure A.4: Script part C

The next part of the script performs the stress and deflection checks. The white and purple group in the top left of this part are the input data for the stress calculations with the floor and layer thickness (white group) and the moments and shear forces for each plank mesh cell (the purple group). The stresses are calculated and checked in four subgroups. The first subgroup A calculates the bending stress in x and y direction and determines which zones should be rotated after which it recalculates the stresses (red part). The next part of subgroup A checks these recalculated stresses to determine if they are below the limits (grey part). Subgroup B has a similar order where the bending stress in the non-rotated zones is calculated (red part) and checked (grey part). Subgroup C calculates the shear force in each layer in the non-rotated zones (red part) and checks these stresses with the corresponding rolling or transverse shear strength (grey part). The final subgroup D first calculates the shear stress in each layer in x and y direction (first red part) and determines if there are additional zones to be rotated based on these results (first grey part). After the rotation the shear stress in each layer in the rotated zones is again calculated (second red part) and checked (second grey part). All subgroups end with a yes or no condition that is looked at when determining of the loop needs to be run for another iteration or not. Subgroup A and D have an additional black group. Of the loop condition of these black replaces the loop condition of the subgroups the optimization is performed without rotating.

The blue group at the bottom of part C is the deflection check. This deflection is automatically checked according to their corresponding span direction by looking at the supports of the floor and determining the relevant span lines.

Part D: loop condition and incrementation

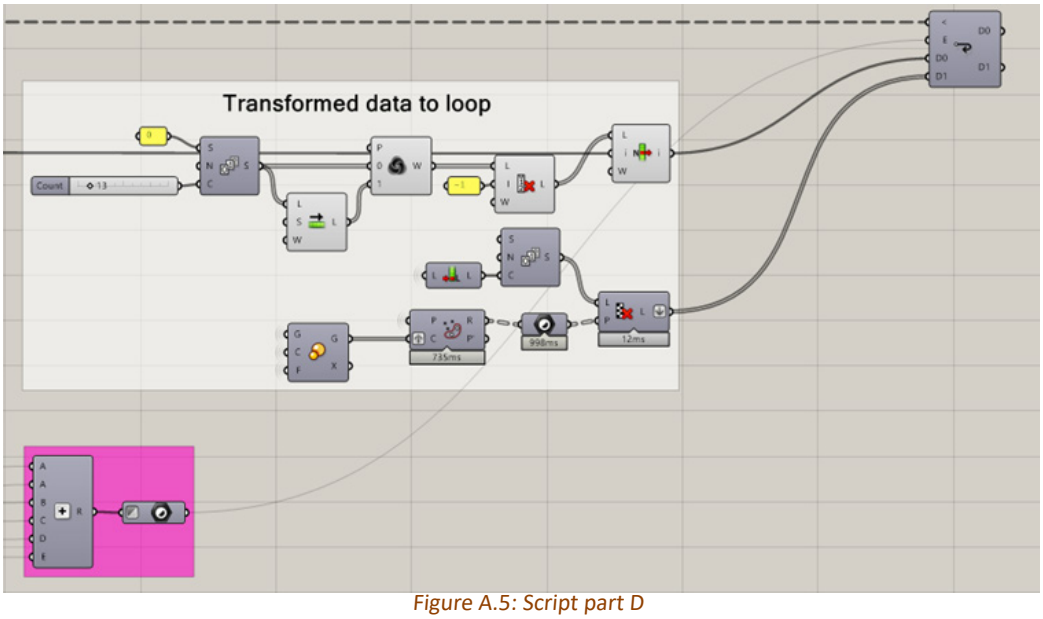

Figure A.5: Script part D

Part D of the script is the end of the loop. The white group in this part is the loop data that is incremented/ changed. This includes increasing the thickness of the floor (loop stream D0) and the zones which are rotated (loop stream D1). The pink group is the loop condition. This part combines all the yes or no conditions of the stresses and deflection checks of part C and only if all checks are satisfied it outputs that the loop can end.

Part E: loop result and plank-layout

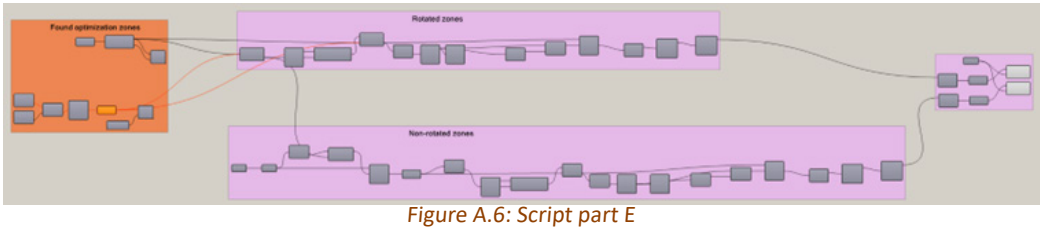

Figure A.6: Script part E

Part E of the script is the final part where the loop results are translated to a plank-layout of the outer layers. The orange group is the results of the loop. This group has two data streams: the rotated zones found based on bending and the rotated zones found based on shear. Again, an orange error bubble can be seen indicating that there is no data flowing through the component. This is again correct as for this case, the optimization did not find any additional rotation zones based on shear stresses. All the required rotation zones were already incorporated into the bending rotation zones.

The following pink groups draw the planks for the rotated zones of the floor (top group) and the non-rotated zones (bottom group) and combines these into a single layer lay-out (final group).

Optimization of Cross Laminated Timber floors through locally varying the major direction based on the geometry, support and loading conditions

Final Mater Thesis

V.B. Staat

Eindhoven University of Technolgy

Eindhoven, June 2023

Thesis layout made using *The Corporate Edition* Indesign template retrieved from symbolt.io